การขจัดโลหะโดยใช้คาร์บอนกัมมันต์-โคบอลต์เฟอร์ไรต์แมกเนติกคอมพอสิต

นางสาวภัทรพร นำศรีนิรันดร์

REMOVAL OF METALS BY ACTIVATED CARBON-COBALT FERRITE MAGNETIC
COMPOSITES

Miss Pattaraporn Numsrinirun

A Thesis Submitted in Partial Fulfillment of the Requirements

for the Degree of Master of Science Program in Chemistry

Department of Chemistry

Faculty of Science

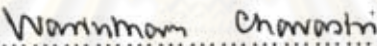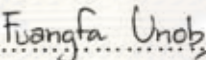Chulalongkorn University

Academic Year 2010

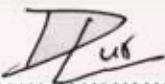| Thesis Title	REMOVAL OF METALS BY ACTIVATED CARBON-COBALT FERRITE MAGNETIC COMPOSITES
By	Miss Pattaraporn Numsrinirun
Field of Study	Chemistry
Thesis Advisor	Assistant Professor Fuangfa Unob, Ph.D.

Accepted by the Faculty of Science, Chulalongkorn University in Partial Fulfillment of the Requirements for the Master's Degree

....Dean of the Faculty of Science

(Professor Supot Hannongbua, Dr.rer.nat.)

THESIS COMMITTEE

....Chairman

(Assistant Professor Warinthorn Chavasiri, Ph.D.)

....Thesis Advisor

(Assistant Professor Fuangfa Unob, Ph.D.)

....Examiner

(Luxsana Dubas, Ph.D.)

....External Examiner

(Assistant Professor Ekasith Somsook, Ph.D.)

iv

ภัทรพร นำศรีนิรันดร์: การขจัดโลหะโดยใช้คาร์บอนกัมมันต์-โคบอลต์เฟอร์ไรต์แมกเนติกคอมพอสิต (REMOVAL OF METALS BY ACTIVATED CARBON-COBALT FERRITE MAGNETIC COMPOSITES) อ.ที่ปรึกษาวิทยานิพนธ์หลัก: ผศ.ดร.เฟื่องฟ้า อุ่นอบ, 69 หน้า.

สังเคราะห์คอมพอสิตคาร์บอนกัมมันต์กับโคบอลต์เฟอร์ไรต์ (AC-CoFe$_2$O$_4$) โดยวิธีการตกตะกอนร่วมทางเคมีเพื่อนำไปใช้ขจัดไอออนโลหะในน้ำ พิสูจน์เอกลักษณ์ด้านสัณฐานวิทยาและข้อมูลพันธะเคมีของวัสดุดูดซับด้วยเทคนิคการเลี้ยวเบนของรังสีเอกซ์ ฟูเรียทรานส์ฟอร์มอินฟราเรดสเปกโทรสโกปี การวิเคราะห์หาพื้นที่ผิว และกล้องจุลทรรศน์อิเล็กตรอนแบบส่องกราด วัสดุคอมพอสิตที่ได้มีการกระจายตัวในน้ำได้ดีขึ้นเมื่อเทียบกับโคบอลต์เฟอร์ไรต์ที่ไม่ได้ทำเป็นคอมพอสิต ศึกษาการดูดซับไอออนโลหะตะกั่ว นิกเกิล และสังกะสี ด้วยระบบแบทช์และหาประสิทธิภาพในการขจัดโลหะดังกล่าวด้วยคอมพอสิตภายใต้อิทธิพลของตัวแปรในสภาวะต่างๆ จากการทดลองพบว่าคอมพอสิต AC-CoFe$_2$O$_4$ มีประสิทธิภาพการขจัดโลหะทั้ง 3 ชนิดมากกว่าวัสดุที่ไม่ได้ทำการคอมพอสิต ระยะเวลาที่เหมาะสมในการขจัดโลหะตะกั่วและนิกเกิล คือ 1 ชั่วโมง และ 2 ชั่วโมงสำหรับสังกะสี และค่าพีเอชที่เหมาะสมในการดูดซับไอออนโลหะ คือ พีเอช 6 และตรวจพบการหลุดออกของโคบอลต์และเหล็กจากคอมพอสิตเมื่อใช้ดูดซับโลหะภายใต้ภาวะพีเอช 1-3 จลศาสตร์การดูดซับเป็นไปตามความสัมพันธ์แบบ Pseudo-second order และพฤติกรรมการดูดซับไอออนโลหะเป็นไปตามสมมติฐานของไอโซเทอร์มแบบแลงเมียร์ ความจุดูดซับสูงสุดของคอมพอสิตในการดูดซับตะกั่ว นิกเกิล และสังกะสี คือ 90.91, 8.06 และ 14.49 มิลลิกรัมต่อกรัม ตามลำดับ ผลของเกลือโซเดียมไนเทรต โซเดียมซัลเฟต และแคลเซียมไนเทรต ที่ความเข้มข้น 0.1 โมลาร์ และ 1.0 โมลาร์ ทำให้ประสิทธิภาพในการขจัดโลหะทุกชนิดลดลง

ศูนย์วิทยทรัพยากร
จุฬาลงกรณ์มหาวิทยาลัย

ภาควิชา _____เคมี_____   ลายมือชื่อนิสิต ......ภัทรพร นำศรีนิรันดร์......

สาขาวิชา _____เคมี_____   ลายมือชื่อ อ.ที่ปรึกษาวิทยานิพนธ์หลัก ....

ปีการศึกษา ____2553____.

5172399823   : MAJOR CHEMISTRY

KEYWORDS: COMPOSITE / ACTIVATED CARBON / COBALT FERRITE / METAL REMOVAL

PATTARAPORN NUMSRINIRUN: REMOVAL OF METALS BY ACTIVATED CARBON-COBALT FERRITE MAGNETIC COMPOSITES. ADVISOR: ASST.PROF. FUANGFA UNOB, Ph.D, 69 pp.

Composite of activated carbon and cobalt ferrite ($AC-CoFe_2O_4$) was synthesized by co-precipitation method for removal of metal ions in water. The prepared adsorbent morphology and chemical bond information was characterized by XRD, FT-IR, surface area analysis and scanning electron microscope. The dispersion of the composite in water was better than non-composite cobalt ferrite. The adsorption studies were performed using batch method and the efficiency in Pb(II), Ni(II) and Zn(II) ions removal were evaluated under influence of certain parameters. The composite $AC-CoFe_2O_4$ showed higher efficiency in removal of all metal ions, compared to non-composite materials. The suitable contact time was 1 hour for removal of Pb(II) and Ni(II) and 2 hour for Zn(II). The suitable pH value for adsorption was 6 and the leaching of cobalt and iron from the composite was observed during adsorption at pH 1-3. The adsorption kinetics followed the pseudo-second order. The adsorption behavior of all metal ions on the composite could be described by Langmuir isotherm assumptions. The maximum capacity of $AC-CoFe_2O_4$ in the adsorption of Pb(II), Ni(II) and Zn(II) were 90.91, 8.06 and 14.49 mg g^{-1}. The presence of salts including sodium nitrate, sodium sulfate and calcium nitrate at 0.1 M and 1.0 M reduced the efficiency in removal of all metal ions by the adsorbent.

Department : ..... Chemistry......   Student's Signature ...... Pattaraporn Numsrinirun ......

Field of Study : ...Chemistry.....   Advisor's Signature ...... Fuangfa Unob ......

Academic Year : ....2010.........

ACKNOWLEDGEMENTS

I would like to thank my advisor, Assistant Professor Dr. Fuangfa Unob for all suggestions, assistance, extreme kindness, forgiveness my mistakes and encouragement. And I would like to thank my appreciation to Assistant Professor Warinthorn Chavasiri, Dr. Luxsana Dubas, and Assistant Professor Dr. Ekasith Somsook for their valuable suggestions as my thesis committees.

This research cannot be completed without the kindness and helps of many people. I would like to thank all of many people in the Environmental Analysis Research Unit for their friendship and good supports. Furthermore, I would like to thank Dr. Amarawan Intasiri and Associate Professor Dr. Thammarat Aree for their suggestion and encouragement. This thesis was financially supported by Center for Petroleum, Petrochemicals and Advanced Materials, Chulalongkorn University.

Finally, I am grateful to my beloved family for their support, entirely care, encouragement and love. The usefulness of this work, I dedicate to my parents and all the teachers who have taught me since my childhood.

CONTENTS

LIST OF TABLES

LIST OF FIGURES

LIST OF SCHEMES

LIST OF ABBREVIATIONS

g	gram
mg	milligram
mol	mole
mmol	millimole
L	liter
mL	milliliter
min.	minute
h.	hour
$^{\circ}$C	degree Celsius
XRD	X-ray diffraction
FT-IR	fourier transform infrared spectrometer
SEM	scanning electron microscope
FAAS	flame atomic absorption spectrometer
FAES	flame atomic emission spectrometer
ICP-OES	inductively couple plasma optical emission spectrometer
USEPA	USA's environmental protection agency
cm^{-1}	wave number unit
$m^2\,g^{-1}$	square meter per gram
$cm^3\,g^{-1}$	square centimeter per gram
M	molar
v/v	volume by volume
w/w	weight by weight
S.D.	standard deviation
PZC	point of zero charge

CHAPTER I

INTRODUCTION

1.1 Statement of the problem

The pollution problem caused by heavy metal has become more severe with the industrial development. Metal industries including refining and electroplating industry generate wastewater containing heavy metal ions. Lead, nickel, and zinc are the metals of environmental and health concern and also found in effluent from these industries [1]. The removal of these metal ions from wastewater before releasing the water to the environment is a requirement. There are several methods for metal removal [2-6] such as chemical precipitation, adsorption, membrane processes and electrochemical process. The adsorption process is one of the most widely used methods for heavy metal ions removal due to its simplicity and convenience. Various adsorbents have been studied and used including activated carbon, silica, zeolite and magnetic particles.

Magnetic particles have become one of the most attractive materials in analytical chemistry [7], biochemistry, medical treatment [8-9]. They are convenience to separate the solid from suspension by applying external magnetic field. Magnetic particles have been used as adsorbents in many applications including metals and dyes removal [10-11] and supported catalyst production [12]. Cobalt ferrite ($CoFe_2O_4$) is one of magnetic compounds that have been widely studied due to its high electromagnetic performance, excellent chemical stability and mechanical hardness [13]. However, the drawback of using magnetic particles as adsorbents is that the magnetic particles always aggregate together resulting in a poor dispersion in water. A decrease in the available surface due to the aggregation may lead to a reduction in the removal efficiency. Therefore, a good dispersion of magnetic particles in water is desired.

Activated carbon is well known as adsorbent and supporter [14-16] due to its high surface area and porosity. It can also disperse well in water under agitation. These properties make it an interesting supporting material. There is a research reporting the coating of magnetic material with silica for solving the aggregation of

pure magnetic particles and using the material to remove organic substances [17]. In this research, activated carbon is used as the support for cobalt ferrite magnetic particles to yield magnetic composite that has good dispersion ability in water. The obtained cobalt ferrite - activate carbon magnetic composite was used for removal of lead, nickel and zinc from water.

1.2 Objective of this work

To synthesize magnetic composite of activated carbon and cobalt ferrite and to investigate the parameters that affect its efficiency in metal removal.

1.3 Scope of this work

The scope of this research was firstly to prepare the composite of activated carbon and cobalt ferrite by co-precipitation method. Secondly, the obtained products were characterized by X-ray diffraction (XRD), scanning electron microscope (SEM), and surface area analysis. In addition, the factors that affect the adsorption of lead, nickel, and zinc ions in solutions were investigated with batch method i.e. stirring time, solution pH, the presence of salts (Na^+, Ca^{2+}, NO_3^-, SO_4^{2-}). Adsorption kinetics and adsorption isotherms were also studied. Finally, the removal of lead, nickel and zinc from an electronic industry wastewater was performed.

1.4 The benefits of this work

To obtain the magnetic composite of activated carbon and cobalt ferrite that can be applied in removal of metal ions in wastewater.

CHAPTER II

THEORY AND LITERATURE REVIEWS

2.1 Magnetic materials [18-19]

Materials are classified by their response when apply the magnetic field. The orientation of electron in magnetic field and the resulting magnetic moment can identify different magnetism of the materials. There are three main classifications of magnetic materials including diamagnetic material, paramagnetic material and ferromagnetic material.

2.1.1 Diamagnetic materials

Diamagnetic materials are weakly repelled by a magnetic field. Completely spin-paired electrons of their subshell oppose the applied field. There is no magnetic susceptibility and the material does not exhibit the magnetic properties when the external field is removed. In diamagnetic materials, there is no permanent net magnetic moment per atom due to paired electrons. The magnetic properties of diamagnetic material arise from the realignment of the electron paths under the influence of an external magnetic field. Diamagnetic elements in the periodic table are copper, silver and gold.

2.1.2 Paramagnetic materials

Paramagnetic materials are affected by magnetic field because of the presence of some unpaired electrons in atoms. There is a small positive magnetic susceptibility and they are slightly attracted to the magnetic field. Moreover, these materials do not retain the magnetic properties when the external field is removed. Paramagnetic elements include magnesium, molybdenum, lithium and tantalum.

2.1.3 Ferromagnetic materials

Ferromagnetic materials exhibit a strong attraction to magnetic field. They have a large and positive magnetic susceptibility. These materials have aligned atomic magnetic moments so they are able to retain their magnetic properties after the

external field is removed. Iron, nickel, and cobalt are examples of ferromagnetic materials.

2.2 Ferrites

Ferrites with AB_2O_4 empirical formula are ferromagnetic materials when A and B are divalent metal ion and trivalent metal ion, respectively. Ferrites according to this formula have cubic spinel structure as shown in Figure 2.1.
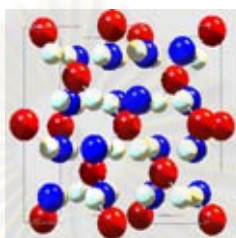
Figure 2.1 Crystal structure of cubic spinel AB_2O_4. Red and blue balls are divalent metal (A) and trivalent metal (B), white are oxygen atoms. [20]

In normal spinel structure, oxygen atoms form a cubic close packed array. In addition, A and B situate in tetrahedral and octahedral sites in the lattice, respectively. On the other hand, an inverse spinel structure is the arrangement which divalent ions (A) are in octahedral sites and the trivalent ions (B) occupy the tetrahedral sites and the rest of octahedral sites. Moreover, almost magnetic materials have inverse spinel structure.

2.2.1 Cobalt ferrite (CoFe$_2$O$_4$)

Among the various ferrite materials, cobalt ferrite is an interesting magnetic compound because it has excellent chemical stability and good mechanical hardness. Crystalline structure of cobalt ferrite is inverse spinel (Figure 2.2).
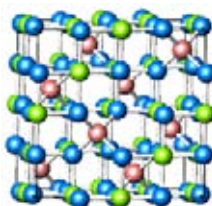
Figure 2.2 Crystal structure of $CoFe_2O_4$ where green balls are Co, pink balls are Fe, and blue balls are O. [21]

2.3 Synthesis of cobalt ferrite

Several methods have been proposed for synthesis of cobalt ferrite as followed.

2.3.1 Sol-gel method [22-23]

The sol-gel techniques for the synthesis of cobalt ferrite use either a mixture of metal nitrate with citric acid solution, or a mixture of metal alkoxides. Then drying techniques are employed for removal of water molecules from the mixture to obtain the brown-colored ashes. Furthermore, when using of citric acid solution in the process, the calcination process was required to remove citric acid from the product resulting in high energy consumption.

2.3.2 Microemulsion method [19]

In microemulsion method, two mixtures of water in oil or two microemulsions are mixed to obtain the metal or metal oxide precipitates. The aqueous phases in the two microemulsions are a solution of metal salt or metal complex and a solution of reducing agent, such as sodium borohydride or hydrazine. The formation is shown in Figure 2.3. This technique needs several chemical reagents to prepare the solutions.
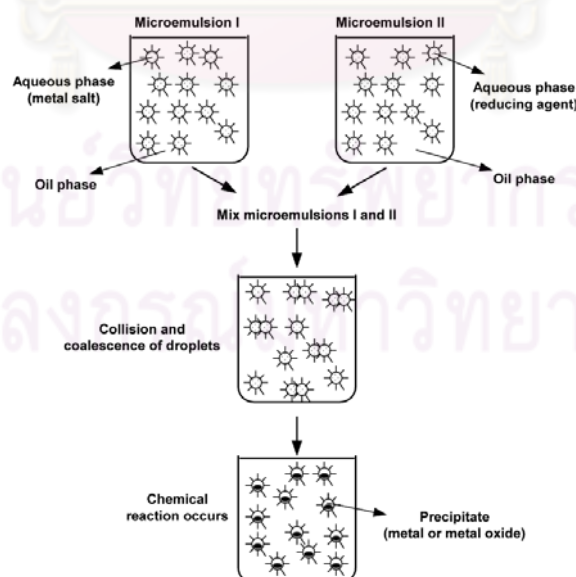
Figure 2.3 Mechanism for the formation of metal particles by microemulsion approach. [19]

2.3.3 Chemical co-precipitation method [24]

Chemical co-coprecipitation method has been widely used for synthesizing cobalt ferrite because of a good reproducibility and controllable stoichiometric composition.

The cobalt ferrite particles are prepared by the chemical co-precipitation method by using Co(II) and Fe(III) solution as starting materials. NaOH is used as the precipitation agent. The stoichiometry of reaction is described by equation 2.1 [24].

$$Co^{2+} + 2Fe^{3+} + 8OH^- \longrightarrow CoFe_2O_4 + 4H_2O \qquad (2.1)$$

2.3.4 Combustion reaction method [25]

In the chemical combustion method, the cobalt ferrite is obtained by the reaction of metal acting as an oxidizing agent and reducing agent including urea, hexamine, glycine, oxalyldihydrazide (ODH), carbohydrazide (CH), tetraformaltrisazine (TFTA), N,N-diformylhydrazine (DFH), etc. as the fuel for the combustion. The reducing agent is mixed with the mixed metal solution of Co^{2+} and Fe^{3+}. The slurry is obtained and heated up to $500^{\circ}C$ for combustion. After water evaporation, the mixed solution has frothed and then ignited for combustion. The solution is evaporated giving out large amount of gases and foamy $CoFe_2O_4$ is obtained as a product. This technique requires several chemical reagents and high energy for combustion process.

Among previously described synthesis methods, the co-precipitation method is often used to synthesize $CoFe_2O_4$ because it is easy to handle and using less chemical reagents. Therefore, the co-precipitation method is chosen to synthesize the $CoFe_2O_4$ in this thesis.

2.4 Activated carbon [26]

Activated carbon is a porous material with porosity enclosed by carbon atoms. Activated carbons are made from hard woods, coconut shell, fruit shell, coals and synthetic macromolecular systems. After carbonization, activation can be performed

through thermal activation by selective gasification for carbon atoms or chemical activation by phosphoric acid.

Activated carbons are used in many applications including the purification and separation of gas mixture. Activated carbon has wide pore size range from micropores to macropores. The application of activated carbons depends on the pore size. For example, activated carbon containing micropores and mesopores are used for adsorption of gas and large molecules, respectively.

<u>Application of activated carbon in aqueous solution</u>

There are many researches reporting the use of activated carbon made from agricultural product for removal of metals, phenolic compounds and organic dyes. For removal of metals, activated carbon was often used as a supporter for the surface modification because it has no specific active sites for metals adsorption. There are reports on the use of the anionic surfactant or organic molecules that contain specific binding site for metal ions impregnated on the activated surface [16, 27].

2.5 Information of lead, nickel and zinc

2.5.1 Lead [28]

Lead is a heavy metal that has atomic number of 82. Metallic Lead is grayish-white color and used in various industries as following. The application of lead in industrial can be devided in two groups.

2.5.1.1 Inorganic lead component

Metallic lead is mixed with other metal for alloys or solder to form plate sheet or wire in chemical industry and filter in communication industry. Oxide of lead is employed in paint industry and battery industry. Salts of lead have several colors, therefore they are often used as primary color pigment in paint industry such as lead chromate (yellow), lead carbonate (white), lead sulfate for toner cartridge, lead acetate for cosmetic industry, lead silicate for ceramic or glazed tiles, lead nitrate for plastic industry and rubber and lead arsenate for pest.

2.5.1.2 Organic lead component

Tetraethyl lead and tetrametyl lead were once used to prevent engine knock. They were mixed in benzene fuel to increase octane number. Organic lead components are more toxic than its inorganic form because they can easily spread in the air while splitting out from the exhaust pipe. So in present, they are not added in the fuel.

2.5.2 Nickel [29]

Nickel is a chemical element that has atomic number of 28. Metallic nickel is silvery-white lustrous. Application of nickel in industrial includes electroplating, catalyst called Raney nickel in hydrogenation reaction of oil, alkaline storage battery, fuel cell electrode and ceramic industry.

2.5.3 Zinc [30]

Zinc is a metallic chemical element that has atomic number of 30. Application of zinc in industrial is various including mining operations, secondary metal production, coal combustion and rubber tire wear and phosphate fertilizers production. Zinc compounds are commonly employed in a variety of product, for example zinc carbonate and zinc gluconate as dietary supplements, zinc chloride in deodorants, zinc pyrithione in anti-dandruff shampoos, zinc sulfide in luminescent paints and zinc methyl or zinc diethyl in the organic laboratory.

2.6 Heavy metal wastewater treatment techniques [31]

In present, wastewater treatment technologies for removal of heavy metal ions include chemical precipitation, ion-exchange, adsorption, membrane filtration and electrochemical treatment.

2.6.1 Chemical precipitation

Chemical precipitation is a widely used process in industry because it is simple and convenient to operate. The conventional chemical precipitation processes are hydroxide precipitation and sulfide precipitation.

2.6.1.1 Hydroxide precipitation

Hydroxide precipitation is the most widely used method because of simplicity, low cost, and ease of pH control. Ca(OH)$_2$ and NaOH are usually used as precipitant for hydroxide precipitation. Furthermore, the minimum pH values for hydroxides precipitation of various metals are in the range of 8.0-11.0. However, the pH for metal hydroxides precipitation depends on the concentration of metal ions. The precipitates can be removed by flocculation and sedimentation.

2.6.1.2 Sulfide precipitation

Sulfide precipitation method is a highly effective method of metal ions removal and it can be operated in a wider pH range compared to hydroxide precipitation. Other advantages of this process include not only lower solubility of metal sulfide compared to hydroxide precipitates but also non-amphoteric property of sulfide precipitates. The process has two steps that are the generation of H$_2$S and metal sulfide precipitation. H$_2$S reacts with divalent metal ions to form insoluble metal sulfides as shown in equation 2.2.

$$M^{2+}{}_{(aq)} + H_2S_{(g)} \rightarrow MS_{(s)} \downarrow + 2H^+{}_{(aq)} \qquad (2.2)$$
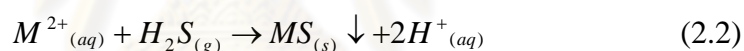
However, the drawback of using sulfide precipitation process is that the toxic H$_2$S fume is formed during the process when heavy metal ions are in acidic media.

2.6.2 Ion exchange

Ion-exchange is the interchange of ions between the counter cations of ion exchangers with the metal ions in the wastewater. Ion exchangers are either cations exchangers that exchange ions of positive charge or anion exchangers that exchange ions of negative charge with other ions of the same charge in water. The most common cation exchangers are strong acid resins and weak acid resins containing sulfonic acid groups (-SO$_3$H) and carboxylic acid groups (-COOH), respectively. When the solution of metal ions passes through the resin, metal ions are exchanged with hydrogen ions on the resin. The mechanisms are shown in equation 2.3 and 2.4.

$$nR - SO_3H + M^{n+} \rightarrow (R - SO_3^-)_n M^{n+} + nH^+ \qquad (2.3)$$

$$nR - COOH + M^{n+} \rightarrow (R - COO^-)_n M^{n+} + nH^+ \qquad (2.4)$$

2.6.3 Adsorption

Adsorption is an effective method for metal ions removal. In addition, metal desorption process leads to adsorbent regeneration and reuse. Various adsorbents are studied and used such as chemically modified activated carbon, agricultural waste, inorganic material and bioadsorbent.

2.6.4 Membrane filtration

Membrane filtration technology shows high efficiency in heavy metal removal. Moreover, this technique is easy to operate and space saving. The different types of membrane processes used to remove metals from the wastewater include ultrafiltration, reverse osmosis, nanofiltration and electrodialysis.

2.6.5 Electrochemical treatment

Electrochemical method is the deposition of metal in elemental form on a cathode surface after electrochemical reduction of metal ions. Electrochemical treatment methods have relatively high operating cost due to the expensive electricity supply, so they have not been widely applied.

2.7 Adsorption [32-33]

Adsorption is the process involving the mass transfer of adsorbates (analytes to be adhered to the surface) from gas phase or liquid phase to the adsorbent surface. Adsorption is generally classified in two types that are physisorption and chemisorption. It will be described in the next sections.

2.7.1 Adsorption process

Adsorption process involves the mass transfer of analytes in liquid or gas phase to the adsorbent surface. It can be divided in three steps as shown in Figure 2.4.
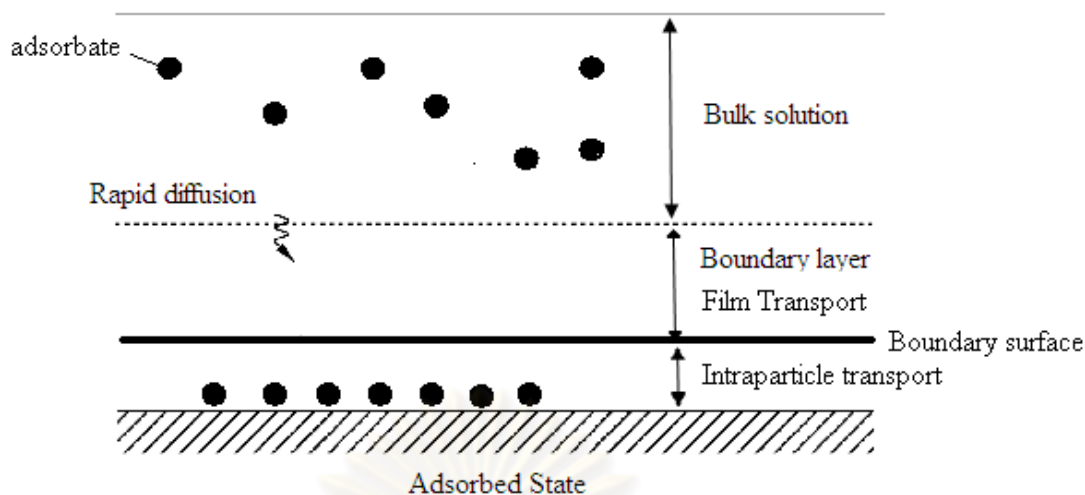
Figure 2.4 The steps of adsorption on the adsorbent surface

2.7.1.1 Bulk transport

This step is a very fast process. The analytes move from the bulk solution to the surface of boundary layer.

2.7.1.2 Film transport

Film transport may occur slowly. This process involves the transportation of analytes from the boundary layer to the surface of adsorbent. It can be called film diffusion or external diffusion.

2.7.1.3 Intraparticle transport

This step is often the rate determining step of the adsorption. The analytes transport from the adsorbent surface to the inside or into the pore of the adsorbent and/or react with the active site. It can be called the internal diffusion.

2.7.2 Physisorption

Physical adsorption is an adsorption process where the attraction between the adsorbates and the adsorbent occurs via van der Waals force or electrostatic interaction without the formation of chemical bond. Moreover, multilayer sorption can occur on the adsorbent surface when the concentration of the adsorbate increases. The reaction of this adsorption is reversible and the active sites on

adsorbent surface are not specific for any analytes. The reversibility of reaction depends on the attraction force of molecules with the active sites, the analyte concentration and temperature.

2.7.3 Chemisorption

Chemisorption occurs when the interaction of the adsorbate and the adsorbent is chemical bond formation, which is stronger than the interaction in physisorption. This process is more specific to the certain groups of analyte due to the specific active site on the adsorbent. Therefore this process is irreversible and only monolayer sorption occurs on these specific active sites.

2.8 Adsorption isotherms [34-35]

Adsorption isotherms are fundamental in describing equilibrium of the analytes adsorption on absorbent surface. The adsorption isotherm expresses the relation between the amount of analyte adsorbed on adsorbent and concentration of analytes in solution at equilibrium. The experimental data are often fit to widely used adsorption isotherm models such as Langmuir and Freundlich models as shown in Figure 2.5 and 2.6.

2.8.1 Langmuir isotherm

The assumption of Langmuir model is based on the adsorption that takes place at specific and homogeneous sites on the adsorbent. The energy of adsorption onto the surface is constant and there is no transmigration of adsorbate on the plane of the surface. The adsorption phenomena are the monolayer adsorption and the maximum adsorption capacity of the adsorbent for that analyte at equilibrium can be predicted. The Langmuir isotherm relationship is expressed as the following equation 2.5.

$$q = \frac{q_m b C_e}{1 + b C_e} \tag{2.5}$$

The equation 2.5 can be written into linear form as shown in equation 2.6,

$$\frac{C_e}{q} = \frac{1}{b q_m} + \frac{C_e}{q_m} \tag{2.6}$$

where q = the amount of solute adsorbed per unit weight of adsorbent at equilibrium (mg g^{-1})

  C_e = the equilibrium concentration of the solute in the bulk solution (mg L^{-1})

  q_m = the maximum adsorption capacity (mg g^{-1})

  b = the constant related to the free energy of adsorption (L mg^{-1})

A plot between C_e / q and C_e yields a straight line with a slope of $1/ q_m$ and intercept of $1/ bq_m$ as shown in Figure 2.5.
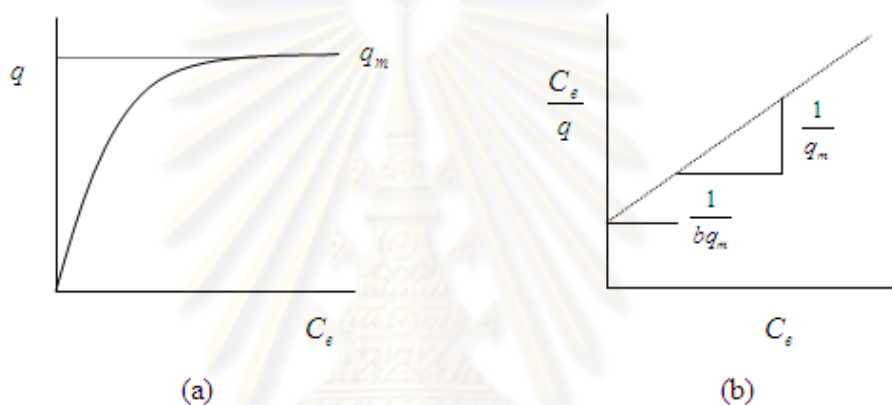
Figure 2.5 The isotherm shape (a) and the linear plot (b) of Langmuir adsorption isotherm [35].

2.8.2 Freundlich isotherm

The Freundlich model was derived by assuming that the adsorption of analytes occurred on heterogeneous surface or surface with active sites of various affinities. The Freundlich model is represented by equation 2.7.

$$q = K_f C_e^{1/n} \tag{2.7}$$

The Freundlich expression is an exponential equation and therefore the linear equation of the Freundlich isotherm is in logarithmic form as shown in equation 2.8,

$$\log q = \log K_f + \frac{1}{n} \log C_e \tag{2.8}$$

where K_f = a constant indicative of the relative adsorption capacity of the adsorbent $(mg\ g^{-1})$

n = a constant indicative of the intensity of the adsorption

A plot between $\log q$ and $\log C_e$ gives a slope of $\dfrac{1}{n}$ and intercept of $\log K_f$ as shown in Figure 2.6.

(a)   (b)
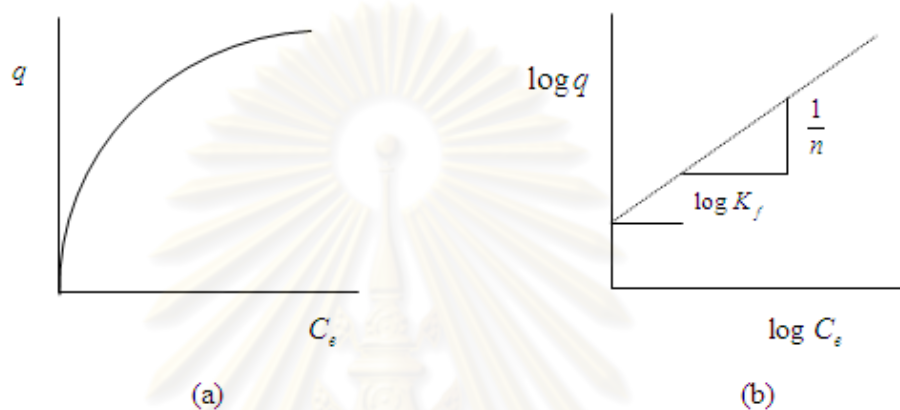
Figure 2.6 The isotherm shape (a) and the linear plot (b) of Freundlich adsorption isotherm [35].

2.9 Literature review

The removal of metals from wastewater by adsorption method has been investigated for many years. Many adsorbents have been developed and the improvement of adsorption efficiency of the adsorbents has also been reported.

Regarding the magnetic materials, there are a few of researches about removal of metal by magnetic materials as shown in Table 2.1. The advantage of using magnetic particles is the ease of solid separation from water by simply using external magnetic field. However, the drawback of using magnetic particles is that it always aggregates together. Therefore, the other substrates (e.g. zeolite, agricultural waste, carbon nanotube, activated carbon) were used and modified with magnetic oxide particles for removal of metal ions. The example of magnetic particles and magnetic materials and their adsorption capacity for metal ions are listed in Table 2.1.

Table 2.1 The adsorption capacity of magnetic particles and magnetic particles
modified materials in metal ions adsorption

Adsorbents	Type of magnetic oxide	Metal ions	Adsorption condition			Ref.
			pH	time	Adsorption capacity(mmol g^{-1})	
Magnetic particles	MnO_2-Fe_3O_4	Cd^{2+}	4	3 h	0.280	[36]
			5	3 h	0.371	
			6	3 h	0.488	
			7	3 h	0.599	
		Ni^{2+}	4	3 h	0.125	
			5	3 h	0.312	
			6	3 h	0.601	
			7	3 h	0.623	
		Pb^{2+}	4	3 h	0.723	
			5	3 h	1.02	
			6	3 h	2.18	
	$NiFe_2O_4$	$Cr_2O_7^{2-}$	5	1 h	0.58	[37]
Magnetic materials **1. zeolite**						
NaY zeolite	Fe_3O_4	Cr^{3+}	5	24 h	0.94	[38]
		Cu^{2+}	5	24 h	1.4	
		Zn^{2+}	5	24 h	1.7	
Synthetic zeolite	Fe_3O_4	Pb^{2+}	5	20 min	0.594	[39]
2. agricultural waste						
- tea waste	Fe_3O_4	Ni^{2+}	4	2 h	0.652	[40]

Table 2.1   (continued)

Adsorbents	Type of magnetic oxide	Metal ions	Adsorption condition			Ref.
			pH	time	Adsorption capacity(mmol g^{-1})	
3. carbon nanotube	Fe_3O_4	Ni^{2+}	6.4	24 h	0.16	[41]

From above information, there were various supporting materials for magnetic particles. Most of the research reported the use of Fe_3O_4 for removal of metal ions. In this work, we are interested in the use of $CoFe_2O_4$ magnetic particles for removal of metal ions.

$CoFe_2O_4$ is a magnetic compound that has high electromagnetic performance, good mechanical hardness and excellent chemical stability. It is an interesting material for the use in removal of metal ions in wastewater. To overcome the problem concerning aggregation of magnetic particles, this thesis focuses on using activated carbon as the supporting material for $CoFe_2O_4$ in order to obtain a magnetic adsorbent that has good dispersion ability in water. The composite of activated carbon-$CoFe_2O_4$ was prepared by co-precipitation method for removal of Pb(II), Ni(II), and Zn(II). The parameters affecting the adsorptions were studied and the most suitable condition was applied for removal of these metals from electronic industry wastewater.

CHAPTER III

EXPERIMENTALS

3.1 Chemicals and instruments

3.1.1 Chemicals

The reagents in all experiments were of analytical grade and summarized in Table 3.1.

Table 3.1 Chemicals and suppliers

Chemicals	Suppliers/Grade
Cobalt nitrate hexahydrate	Asia pacific specially chemicals, Australia / for analysis
Ferric chloride	Merck, Germany / for analysis
Lead standard solution	Merck, Germany / for analysis
Nickel standard solution	Merck, Germany / for analysis
Iron standard solution	Merck, Germany / for analysis
Cobalt standard solution	Merck, Germany / for analysis
Sodium acetate	Merck, Germany / for analysis
Sodium hydroxide	Merck, Germany / for analysis
Sodium nitrate	CARLO ERBA, Italy / GR ACS
Sodium sulfate	Merck, Germany / for analysis
Calcium nitrate	Riedel-de Haën®, Germany / for analysis
Nitric acid 65% w/w	Merck, Germany / for analysis
Activated carbon powder	Merck, Germany / for analysis

3.1.2 Instruments

All instruments used in the experiment are listed in the Table 3.2.

Table 3.2   List of instruments

Instruments	Manufacture : Model
Stirrer/Hot plate	CORNING : PC-420 and PC-620.
Oven	Memmert : UM 500
Vacuum pump	Buchi : V-700
pH meter	Hanna instruments : pH 211
Micropipette	Brand : 10-100 µL, 100-1000 µL
X-ray diffractometer	Rigaku : 1200+
Scanning electron microscope	Jeol : JSM 5800
Surface area analyzer	BEL Japan : BELSORP-mini
Flame atomic absorption spectrometer (FAAS)	Perkin Elmer : AAnalyst 100
Fourier transform infrared spectrometer (FT-IR)	Thermo Fisher : Nicolet iS10
Inductively coupled plasma-optical emission spectrometer (ICP-OES)	Thermo scientific : iCAP 6000

3.2 Preparation of chemical solutions

3.2.1 Working standard lead solutions

Working standard lead solutions of 3, 6, 9, 15 and 18 mg L^{-1} were prepared by dilution of lead standard solution (1000 mg L^{-1}). A volume of 30, 60, 90, 150 or 180 µL of lead standard solution was transferred into a 10.00 mL volumetric flask and then, the volume was made up to the mark with deionized water**.**

3.2.2 Working standard nickel solutions

Working standard nickel solutions of 2, 4, 6, 8 and 10 mg L^{-1} were prepared by dilution of nickel standard solution (1000 mg L^{-1}). A volume of 20, 40 ,60, 80 or 100 µL of nickel standard solution was transferred into a 10.00 mL volumetric flask and then, the volume was made up to the mark with deionized water**.**

3.2.3 Working standard zinc solutions

The standard zinc solution of 10 mg L^{-1} was prepared by pipetting 250 µL of zinc standard solution (1000 mg L^{-1}) into a 25.00 mL volumetric flask and adjusting the volume to the mark with deionized water.

Working standard zinc solutions of 0.2, 0.4, 0.6, 0.8 and 1.0 mg L^{-1} were prepared by dilution of zinc standard solution (10 mg L^{-1}).A volume of 200,400 ,600, 800 or 1000 µL of the zinc standard solution was transferred into a 10.00 mL volumetric flask and then, the volume was made up to the mark with deionized water.

3.2.4 Nitric acid solutions

Nitric acid solutions (1, 5 and 10% v/v) for pH adjustment and nitric acid solution (5 M) for oxidizing activated carbon were prepared by direct dilution of the concentrated nitric acid solution (65% w/w).

3.2.5 Sodium hydroxide solutions

Sodium hydroxide solutions (1, 5 and 10% v/v) for pH adjustment and sodium hydroxide solution (3.5% w/v) for co-precipitation of cobalt ferrite were prepared by dissolving the appropriate amount of NaOH in deionized water.

3.2.6 Sodium acetate solution

Sodium acetate solution (0.005 M) was prepared by dissolving the appropriate amount of CH_3COONa in deionized water.

3.2.7 Sodium nitrate solution

Sodium nitrate solution (0.005 M) was prepared by dissolving the appropriate amount of $NaNO_3$ in deionized water.

3.2.8 Metal solutions containing different salts

The metal solutions containing different salts (sodium nitrate, sodium sulfate or calcium nitrate) of 0.1 M and 1 M used in the study of salt effect were prepared by dissolving the appropriate amount of the salts: sodium nitrate, sodium sulfate or calcium nitrate with 50 mg L^{-1} of Pb(II), 10 mg L^{-1} of Ni(II) or 5 mg L^{-1} of Zn(II) solutions in deionized water.

3.3 Synthesis of cobalt ferrite (CoFe$_2$O$_4$) and composite of activated carbon and cobalt ferrite (AC-CoFe$_2$O$_4$)

3.3.1 Synthesis of cobalt ferrite (CoFe$_2$O$_4$)

The synthesis procedure was adapted from the method proposed by Ai et.al [42]. Sodium hydroxide solution (3.5 %w/v, 100 mL) was heated to 90°C under electromagnetic stirring. Then, cobalt nitrate hexahydrate (1.450 g, 0.005 mol) and ferric chloride (1.622 g, 0.010 mol) were dissolved in 50 mL deionized water. This mixed metal solution was added dropwise into the NaOH solution and continuously stirred at 90°C for 2 h. The solid product was recovered by filtration and dried in the oven for 16 h. The obtained product was washed with deionized water until the pH of filtrate was neutral.
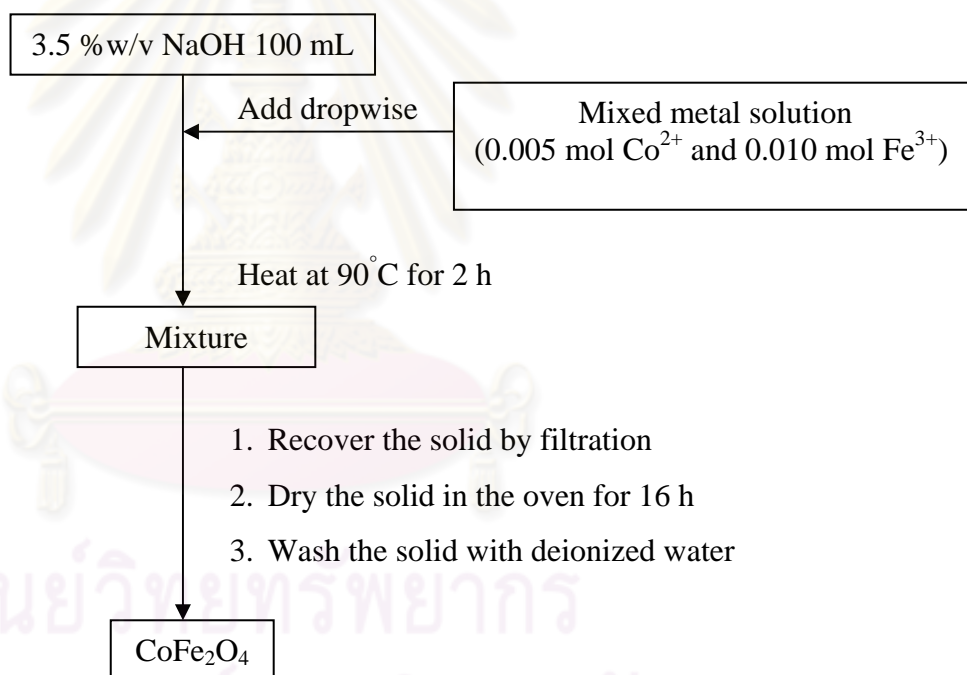
Scheme 3.1 Procedure of CoFe$_2$O$_4$ synthesis.

3.3.2 Synthesis of composite activated carbon and cobalt ferrite (AC-CoFe$_2$O$_4$)

The synthesis of composite AC- CoFe$_2$O$_4$ was divided in two steps.

3.3.2.1 <u>Preparation of activated carbon</u>

An amount of 3 g of activated carbon was oxidized by 5 M nitric 100 mL for 3 h. Then, the oxidized activated carbon was washed with deionized water until the pH of filtrate was neutral.

3.3.2.2 <u>Preparation of composite of AC- CoFe$_2$O$_4$</u>

The method for AC-CoFe$_2$O$_4$ synthesis is very similar to the method of CoFe$_2$O$_4$ synthesis. The difference is that the oxidized activated carbon was mixed with NaOH solution prior to the addition of the mixed metal solution as shown in scheme 3.2.

```
┌──────────────────────────────┐      ┌──────────────────────────┐
│ 1 g oxidized activated carbon│  +   │ 3.5 %w/v NaOH 100 mL     │
└──────────────────────────────┘      └──────────────────────────┘

                  Add dropwise        ┌──────────────────────────────────────┐
                  ◄───────────────────│ Mixed metal solution                 │
                                      │ (0.005 mol Co²⁺ and 0.01 mol Fe³⁺)  │
                                      └──────────────────────────────────────┘

                  Heat at 90°C for 2 h
           ┌──────────────┐
           │   Mixture    │
           └──────────────┘

                      1. Recover the solid by filtration
                      2. Dry the solid in the oven for 16 h
                      3. Wash the solid with deionized water

           ┌──────────────┐
           │ AC-CoFe₂O₄   │
           └──────────────┘
```
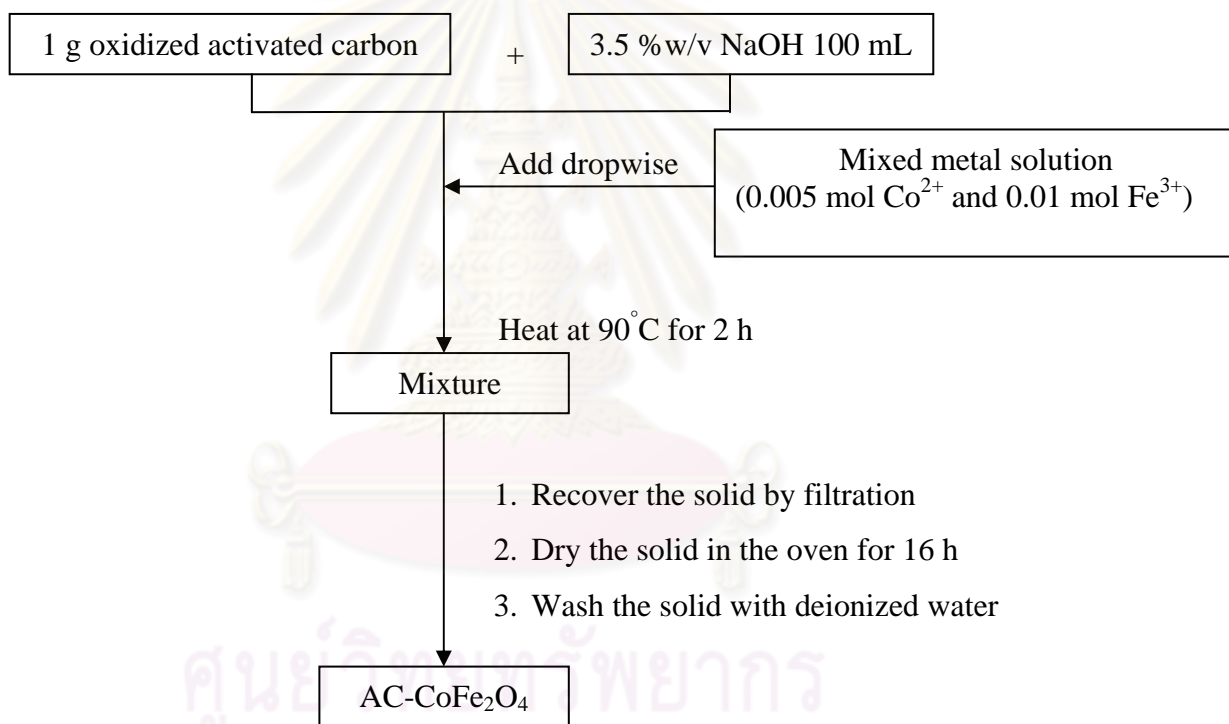
Scheme 3.2 Procedure of AC-CoFe$_2$O$_4$ synthesis.

3.4 Characterization of the adsorbents

The instruments and techniques used to characterize the adsorbents are described in the following part.

3.4.1 X-ray diffraction (XRD)

The structure of synthesized materials were identified by a Rigaku D/MAX-220 Ultima+ X-ray diffractometer (XRD) equipped with Cu K$_\alpha$ radiation (40 kV 30 mA) and a monochromater at 2 theta angle between 20 to 70 degrees. The scattering slit, divergent slit and receiving slit were fixed at 0.5 degree, 0.5 degree, and 0.15 mm, respectively. X-ray diffraction patterns provide the information about the structure and crystallization of $CoFe_2O_4$ and $AC-CoFe_2O_4$.

3.4.2 Fourier transform infrared spectroscopy (FT-IR)

Fourier transform infrared spectra were recorded on Nicolet FT-IR impact iS10 spectrophotometer. The solid samples were prepared by pressing the sample with KBr. Infrared spectra were recorded between 400 cm^{-1} to 4,500 cm^{-1} in transmittance mode. The FT-IR technique was used to characterize functional groups of $CoFe_2O_4$ and $AC-CoFe_2O_4$.

3.4.3 Nitrogen adsorption (Brunauer-Emmett-Teller method (BET))

The determination of BET specific surface area and total pore volume of the adsorbents were performed using a surface analyser (BEL Japan, BELSORP-mini instrument). The sample weight was about 20 mg. Then, the sample was weighed exactly after pretreatment at $400^\circ C$ for 3 h before each measurement. The principle of this method is the adsorption of N_2 gas by $AC-CoFe_2O_4$. Sample adsorbed the N_2 gas by following monolayer adsorption. The amount of adsorbed sample directly gave the total surface area of sample.

3.4.4 Scanning electron microscope (SEM)

The images of sample surface were collected by using a scanning electron microscope (Jeol :JSM 5800). A high energy electron beam from the electron microscope interacts with the atoms in sample producing signals that contain information about the sample surface topography.

3.5 Adsorption studies

The adsorption of Pb(II), Ni(II) and Zn(II) ions in aqueous solutions by activated carbon, $CoFe_2O_4$, and $AC-CoFe_2O_4$ was studied using batch method. The amount of adsorbent was 0.0100 g for adsorption of metal ions in 10.00 mL solution. The adsorbents were separated by using external magnetic field. The initial and residual concentrations of metal ions in solution were determined by FAAS. All experiments were performed in triplicate. The ionic strength of the metal ions solution was controlled by 0.005 M $NaNO_3$ or 0.005 M CH_3COOH.

3.5.1 Comparison of adsorption of activated carbon, $CoFe_2O_4$, and $AC-CoFe_2O_4$

The efficiency in metal ions adsorption by three adsorbents including activated carbon, $CoFe_2O_4$, and $AC-CoFe_2O_4$ were evaluated. The initial concentration of Pb(II) in 0.005M CH_3COONa, Ni(II) and Zn(II) in 0.005 M $NaNO_3$ were 30 mg L^{-1}, 30 mg L^{-1} and 20 mg L^{-1}, respectively.

3.5.2 Effect of contact time

The effect of contact time on metal ions adsorption by $AC-CoFe_2O_4$ was investigated by varying time in the range of 30 – 240 min. The solution pH was 4.0 ± 0.2. The initial concentration of Pb(II) in 0.005 M CH_3COONa, Ni(II) and Zn(II) in 0.005 M $NaNO_3$ were 50 mg L^{-1}, 30 mg L^{-1} and 20 mg L^{-1}, respectively.

3.5.3 Effect of pH

The effect of the solution pH on the metal ions adsorption by $AC-CoFe_2O_4$ was investigated in the pH range of 1-6 and pH higher than 6 caused precipitation of metal ions. The pH adjustment was carried out using sodium hydroxide solutions (1, 5, or 10 %v/v) and nitric acid solutions (1, 5, or 10 % v/v). The contact time was 180 min. The metal ions solution prepared in 0.005 M CH_3COONa contained 50 mg L^{-1} Pb(II), 30 mg L^{-1} Ni(II) or 20 mg L^{-1} Zn(II).

3.5.4 Leaching of CoFe$_2$O$_4$ during adsorption

The leaching of Co and Fe from composite AC-CoFe$_2$O$_4$ during adsorption was evaluated at different solution pH. The amount of Co and Fe found in solution at different pH were determined and compared with the total amount of Co and Fe in the composite. The Co and Fe content in the composite was determined by acid digestion following standard method 3050B of USEPA (United States Environmental Protecting Agency) [43].

3.5.5 Adsorption kinetics and effect of adsorbent dosage

The adsorption kinetics and the effect of adsorbent dose was studied at room temperature (28 ± 2°C) by observing the adsorption capacity of AC-CoFe$_2$O$_4$ when varied the contact time from 5 to 120 min with the adsorbent dose in the range of 0.01 to 0.04 g of AC-CoFe$_2$O$_4$. The 50 mg L^{-1} of Pb(II), 10 mg L^{-1} of Ni(II) or 5 mg L^{-1} of Zn(II) solution was prepared under 0.005 M CH$_3$COONa at pH 5, 6 and 6, respectively.

3.5.6 Adsorption isotherms

The adsorption isotherms were studied at 28°C by varying the initial metal concentration from 1 to 400 mg L^{-1}. The experimental results were fitted with Langmuir and Freundlich adsorption model to describe the adsorption equilibrium at the solid-liquid interface and estimate the maximum capacity of the AC-CoFe$_2$O$_4$ in metal ion adsorption.

Metal ion solutions were prepared in 0.005 M CH$_3$COONa at pH 5, 6 and 6 for Pb(II), Ni(II) and Zn(II), respectively. The contact time was 180 min to assure that the maximum adsorption capacity was reached.

3.5.7 Effect of salt

The effect of salt were studied by adding the NaNO$_3$, NaSO$_4$ or Ca(NO$_3$)$_2$ in the concentration of 0.1 or 1.0 M in the metal ions solution. The 50 mg L^{-1} of Pb(II), 10 mg L^{-1} of Ni(II) or 5 mg L^{-1} of Zn(II) solution was prepared under 0.005 M CH$_3$COONa at pH 5, 6, and 6 respectively. The contact time was 120 min.

3.6 Application to wastewater sample from battery factory

The wastewater samples employed in this study were collected from a battery factory. The AC-CoFe$_2$O$_4$ was applied to remove Pb(II), Ni(II), and Zn(II) ions from the wastewater. Before using in adsorption experiments, the wastewater was filtered and the pH of the sample was measured. The wastewater was analyzed for metal ions in the solution with ICP-OES. Then, the initial concentration of the studied metal ions (Pb(II), Ni(II) and Zn(II)) were determined by FAAS. The pH of the sample was adjusted to pH 6 with 1, 5 or 10% v/v sodium hydroxide prior to the application in adsorption experiment. The contact time was 120 min.

CHAPTER IV

RESULTS AND DISCUSSION

4.1 Synthesis of cobalt ferrite ($CoFe_2O_4$) and composite of activated carbon and cobalt ferrite ($AC-CoFe_2O_4$)

$CoFe_2O_4$ and $AC-CoFe_2O_4$ were synthesized by co-precipitation method using Co(II) and Fe(III) salts as starting materials. The molar ratio of Co(II) and Fe(III) was 1:2 and sodium hydroxide was used as precipitant. The obtained products had magnetic property as shown in Figure 4.1. Furthermore, $AC-CoFe_2O_4$ could disperse in aqueous solution better than $CoFe_2O_4$ as shown in Figure 4.2. The better dispersion of adsorbents in water may result in higher efficiency in metal removal. The efficiency in metal adsorption by $CoFe_2O_4$ and $AC-CoFe_2O_4$ was further investigated.

(a)   **(b)**
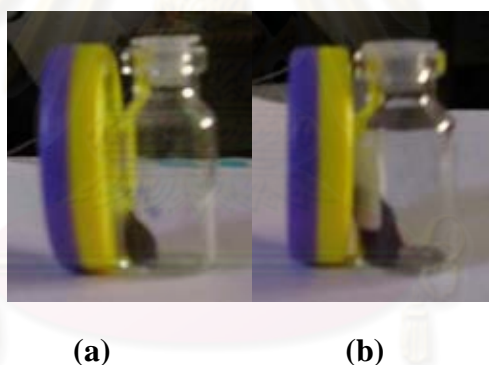
Figure 4.1 Magnetic property of (a) $CoFe_2O_4$ and (b) $AC-CoFe_2O_4$.

(a)   (b)

Figure 4.2 Dispersion of (a) $CoFe_2O_4$ and (b) $AC-CoFe_2O_4$ in water.

The amount of $CoFe_2O_4$ in the composite was determined by measuring the content of Fe and Co in the composite. The amount of Fe and Co found in the composite was 0.2536 g (4.54 mmol) and 0.1318 g (2.24 mmol) per one gram of composite, respectively. The mole ratio of Fe to Co was 2:1 which was in agreement of theoretical ratio in $CoFe_2O_4$ formation. Therefore, the amount of $CoFe_2O_4$ in the composite was 2.24 mmoles or 0.5246 gram per gram of composite. This result shows that the composite contained $CoFe_2O_4$ half of composite weight.

4.2 Characterization of adsorbents

4.2.1 X-ray diffraction technique (XRD)

X-ray diffraction technique was used to characterize the structure of $CoFe_2O_4$ and $AC-CoFe_2O_4$, compared to activated carbon. The results are shown in Figure 4.3. The XRD board peak of activated carbon appeared at 2θ of $26.4°$ and a sharper diffraction peak at $43.2°$. These results are in agreement with the XRD pattern of the C-graphite (JCPDS card no. 99-0057).
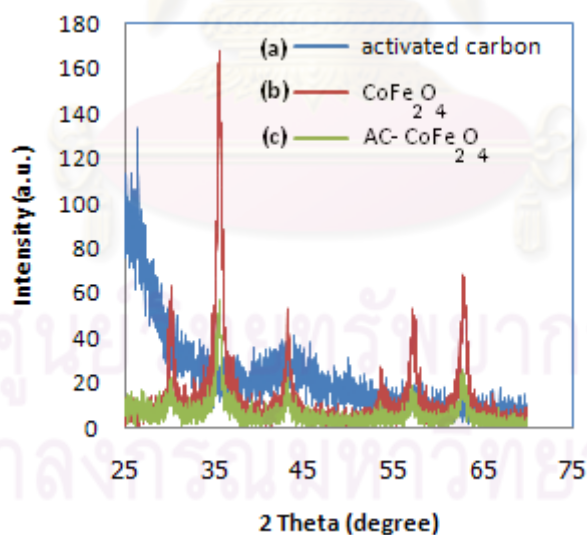
Figure 4.3 XRD patterns of (a) activated carbon, (b) $CoFe_2O_4$ and (c) $AC-CoFe_2O_4$.

Regarding the XRD pattern of $CoFe_2O_4$ and $AC-CoFe_2O_4$, the peaks of the both patterns appeared at 2θ of $30.3°$, $35.6°$, $43.1°$, $53.6°$, $57.2°$ and $62.9°$ indicating the cubic spinel structure of $CoFe_2O_4$ (JCPDS card no. 22-1086). The XRD

pattern of AC-CoFe$_2$O$_4$ is identical to that of CoFe$_2$O$_4$ particles, revealing that the composite contained the magnetic particles. However, AC-CoFe$_2$O$_4$ showed lower peak intensity and the characteristic peak of activated carbon at 26.4° disappeared.

4.2.2 Fourier transform infrared spectroscopy (FT-IR)

Fourier transform infrared spectroscopy (FT-IR) was used to confirm the presence of magnetic particles in the composites by observing the signal of characteristic bond of magnetic particles i.e. Fe-O.

The FT-IR spectra of activated carbon, CoFe$_2$O$_4$ and AC-CoFe$_2$O$_4$ are shown in Figure 4.4. The IR spectra of activated carbon showed peaks at 3400, 2300, 1700 and 1100 cm^{-1}. The O-H bond stretching band of adsorbed water molecule was observed in spectrum at 3410 cm^{-1}. The signal at 2300 cm^{-1} was attributed to ketone groups. The peak at about 1700 cm^{-1} could be assigned to carboxylic group and the C-O bond stretching band of carboxylic group was observed at 1062 cm^{-1}. The weak signal at about 900-600 cm^{-1} was the C-C rocking band of activated carbon [44]. The CoFe$_2$O$_4$ showed the IR signal at 594.76 cm^{-1} which was the Fe-O vibration band [45].
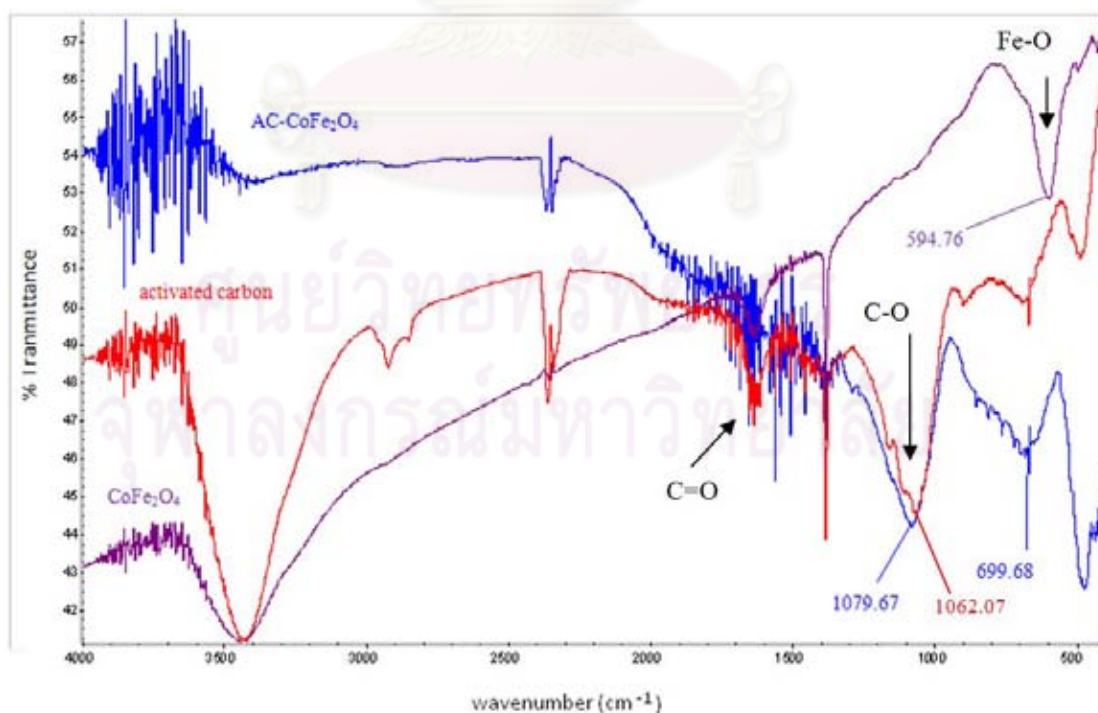
Figure 4.4 FT-IR spectra of activated carbon, CoFe$_2$O$_4$ and AC-CoFe$_2$O$_4$.

According to Figure 4.4, the IR spectrum of AC-CoFe$_2$O$_4$ was almost identical to that of the activated carbon. This result shows that the activated carbon was also present in the composite, even though it was not seen in the XRD pattern of the composite as shown previously. However, it was not observed clearly the signal of Fe-O vibration in the AC-CoFe$_2$O$_4$ IR spectra. It is probably due to the overlap of Fe-O band and C-C rocking band of activated carbon.

4.2.3 Surface area analysis

Surface area analysis was performed by N$_2$ adsorption using Brunauer-Emmett-Teller method (BET) in order to compare the surface area and total pore volume of activated carbon, CoFe$_2$O$_4$ and AC-CoFe$_2$O$_4$. The results are shown in Table 4.1.

Table 4.1 Surface area and total pore volume of activated carbon, CoFe$_2$O$_4$
and AC-CoFe$_2$O$_4$ composite

Adsorbents	BET-surface area (m^2 g^{-1})	Total pore volume (cm^3 g^{-1})
Activated carbon	755	0.59
CoFe$_2$O$_4$	77	0.16
AC- CoFe$_2$O$_4$	276	0.27

From Table 4.1, the results show that the surface area and the pore volume of activated carbon were higher than those of CoFe$_2$O$_4$ and the composite. The surface area of the composite of activated carbon and CoFe$_2$O$_4$ was 276 m^2 g^{-1} which was relatively low, compared to that of the activated carbon. This result could be explained that the surface of activated carbon in the composite was covered by CoFe$_2$O$_4$ particles and these particles may block the pores of activated carbon. In addition, CoFe$_2$O$_4$ is a non-porous material so the surface area and pore volume of the resulting composite were reduced.

4.2.4 Scanning electron microscope (SEM)

Scanning electron microscope was used to exhibit the surface morphology of activated carbon, $CoFe_2O_4$ and $AC\text{-}CoFe_2O_4$ (Figure 4.5). It can be noticed that the non composite $CoFe_2O_4$ (Figure 4.5 b) have various particles size in the range of 10-200 µm. On the other hand, the composite $AC\text{-}CoFe_2O_4$ had irregular form with narrower range of particle size. The particles size of the composite was similar to activated carbon particles.
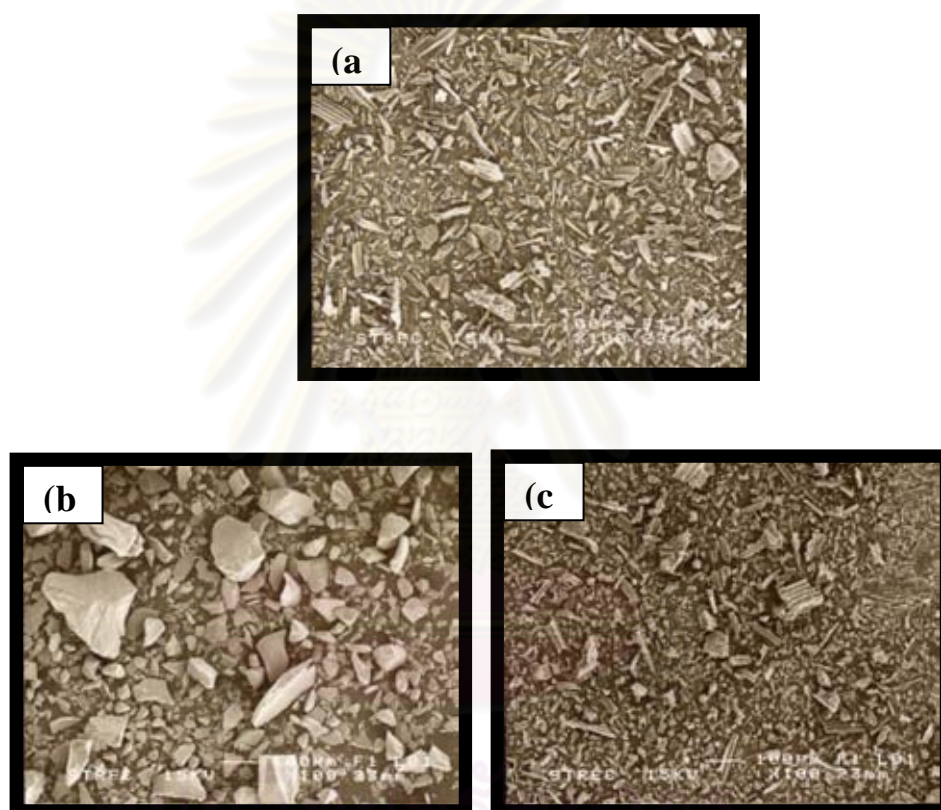
Figure 4.5 The SEM micrograph of (a) activated carbon (b) $CoFe_2O_4$ and (c) $AC\text{-}CoFe_2O_4$. ($\times$100)

From Figure 4.6 (a), there are many pores on activated carbon and the surface of activated carbon is clear and smooth. After making a composite of activated carbon and $CoFe_2O_4$, it can be seen that the surface and pore of activated carbon was covered with magnetic particles that had irregular shape (blue circle). This observation confirms the surface area analysis results that the surface area and total

pore volume of the composite were lower than those of non composite activated carbon because of the coverage of magnetic particles on activated carbon surface. However, the $CoFe_2O_4$ particles that did not attach to activated carbon surface (red circle) were also observed.
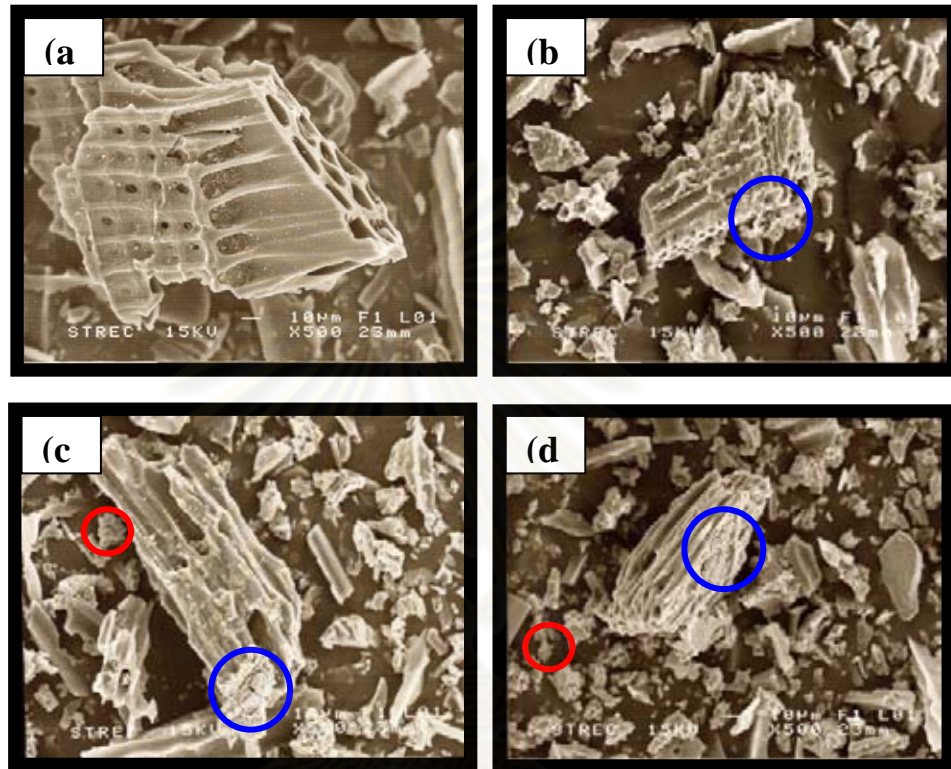
Figure 4.6 The SEM micrographs of (a) activated carbon ($\times$500), (b)-(d)
AC- $CoFe_2O_4$. ($\times$500)

4.3 Adsorption studies

4.3.1 Comparison of adsorption efficiency of activated carbon, $CoFe_2O_4$ and AC-$CoFe_2O_4$

The metal ions adsorption experiments were performed using activated carbon, $CoFe_2O_4$ and AC-$CoFe_2O_4$ to compare the efficiency in metal removal by these adsorbents. The results are shown in Figure 4.7.
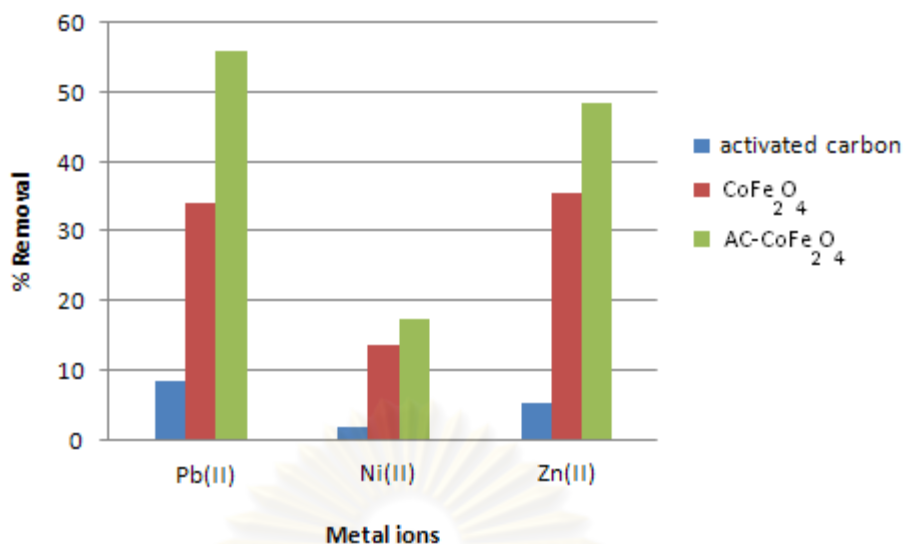
Figure 4.7 Comparison of adsorbents in the removal of Pb(II), Ni(II) and Zn(II). (0.01
g adsorbent, 10 mL metal solution (Pb(II) 50 mg L^{-1}, Ni(II) 30 mg L^{-1} or
Zn(II) 20 mg L^{-1}), pH 4)

The metal ions adsorption efficiency and the removal efficiency was in
the order of AC-CoFe$_2$O$_4$ > CoFe$_2$O$_4$ > activated carbon under the same experimental
conditions. The activated carbon showed low efficiency in metal removal while
CoFe$_2$O$_4$ had much higher efficiency due to the higher number of active sites (i.e. OH
groups). In addition, the results indicate that the AC-CoFe$_2$O$_4$ showed the highest
efficiency, compared to activated carbon and CoFe$_2$O$_4$. Regarding the content of
CoFe$_2$O$_4$ in the composite determined previously, about 50% by weight of composite
was CoFe$_2$O$_4$. Even though the composite contained lower amount of CoFe$_2$O$_4$, it still
showed higher efficiency in metal removal than the non composite CoFe$_2$O$_4$ when
used the same adsorbent weight in the adsorption (e.g. 0.01 g CoFe$_2$O$_4$ or 0.01 g AC-
CoFe$_2$O$_4$ in this study). This result could be explained by a better dispersion of the
composite AC-CoFe$_2$O$_4$ in water, compared to non composite CoFe$_2$O$_4$. It is also
possible that the number of available active sites for metal ions adsorption in non
composite CoFe$_2$O$_4$ was less than in the AC-CoFe$_2$O$_4$ because of the particles
aggregation.

4.3.2 Effect of contact time

In this experiment, the effect of contact time was studied and the time to reach the adsorption equilibrium was determined for the use in further experiments. The amount of Pb(II), Ni(II) and Zn(II) ions adsorbed on AC-CoFe$_2$O$_4$ at different contact time are shown in Figure 4.8.
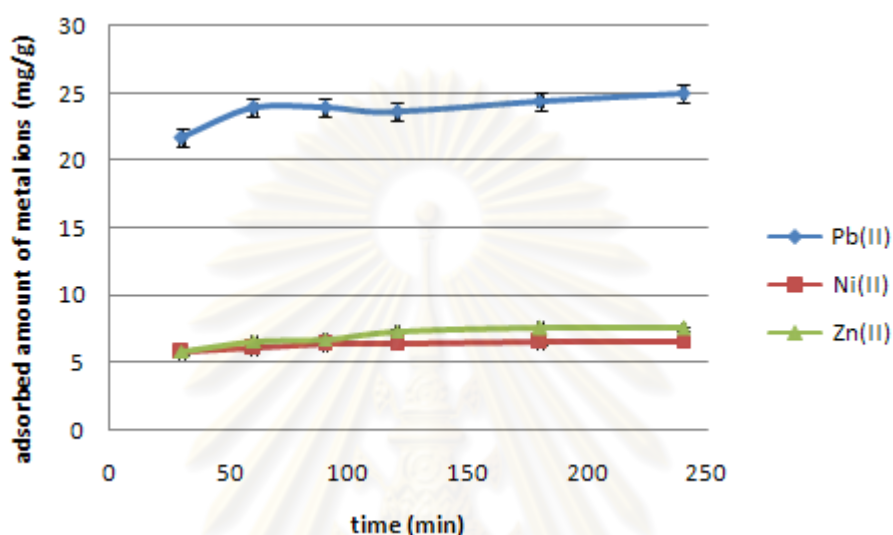
Figure 4.8 Effect of contact time on the adsorption of Pb(II), Ni(II) and Zn(II) by AC-CoFe$_2$O$_4$. (0.01 g adsorbent, 10 mL metal solution (Pb(II) 50 mg L^{-1}, Ni(II) 30 mg L^{-1} or Zn(II) 20 mg L^{-1}), pH 4)

The results show that the adsorption efficiency increased in increasing the contact time before reaching relatively constant values. According to the graph in Figure 4.8, it is difficult to decide when the adsorption reached the equilibrium. One-way analysis of variance (ANOVA) was used to test the effect of contact time. No significant difference in adsorption efficiency was found at 60 min and longer contact time for Pb(II) and Ni(II) and at 120 min and longer contact time for Zn(II). The results of statistical analysis are shown in Table B1-B9 (see appendix). The contact time of 180 min was chosen for further adsorption experiments to assure that the adsorption equilibrium was reached.

4.3.3 Effect of pH

The pH of solution could have strong influence on the metal adsorption on the adsorbent due to the protonation/deprotonation of active sites on surface of the adsorbents at different pH. In this work, the pH of solution was studied in the range of 1-6 because at higher pH values, metal ions could be removed by precipitation as metal hydroxide. The effect of pH on the removal of Pb(II), Ni(II) and Zn(II) ions by AC-CoFe$_2$O$_4$ are shown Figure 4.9.
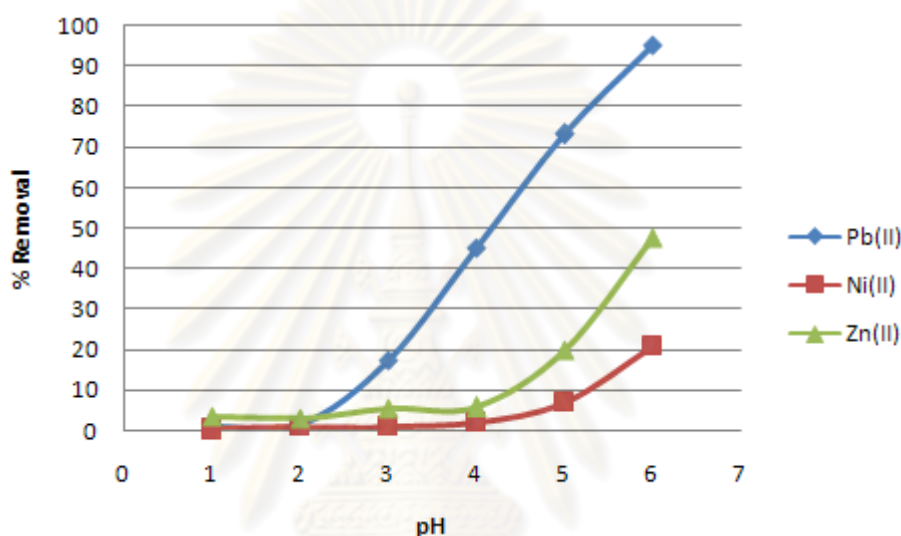
Figure 4.9 Effect of pH on the removal of Pb(II), Ni(II) and Zn(II) using
AC-CoFe$_2$O$_4$ (0.01 g adsorbent, 10 mL metal solutions (Pb(II) 50 mg L^{-1},
Ni(II) 30 mg L^{-1} or Zn(II) 20 mg L^{-1})

From Figure 4.9, the removal of all metal ions obviously increased with increasing of solution pH from 1 to 6. Similar trends were observed for all metal ions. The suitable pH for all metals removal was pH 6. However, when the concentration increases, the mechanism in metal removal at this chosen pH could be the result of both adsorption and hydroxide precipitation.

The nature of functional groups on adsorbent and pH of solution can affect the metal ions adsorption on adsorbent. At low pH values, the H$^+$ concentration increases and may compete with metal cations to adsorb on surface hydroxyl group of AC-CoFe$_2$O$_4$. When the AC-CoFe$_2$O$_4$ surface was protonated by H$^+$, it is difficult for metal cations to further adsorb at the positively charged active sites via electrostatic

interaction due to electrostatic repulsion. Regarding the pH_{PZC} of $CoFe_2O_4$ (pH_{PZC} of $CoFe_2O_4 = 8.0$) [46], when the pH of solution is lower than 8.0, the hydroxyl groups on $CoFe_2O_4$ surface of the composite is positively charged. On the other hand, in solutions having pH value above pH_{PZC}, the surface hydroxyl groups are negatively charged and the adsorption of metal cations may take place via electrostatic interaction. However, the solution pH in this study was lower than 8.0, so the removal of metal ions would not occur via electrostatic interaction. The possible mechanism for metal ion removal by AC-$CoFe_2O_4$ is shown in equation 4.1 [47], when >SOH represents surface hydroxyl group.

$$>SOH + M^{2+}_{(aq)} \rightarrow >SOM^+ + H^+_{(aq)} \qquad (4.1)$$

At higher pH values, less H^+ amount would protonate on the surface hydroxyl groups of AC-$CoFe_2O_4$ resulting in higher number of hydroxyl species (>SOH) on the surface. Therefore, the metal adsorption occurred and the removal efficiency increased.

Moreover, decreasing of $CoFe_2O_4$ amount on AC-$CoFe_2O_4$ due to the dissolution of $CoFe_2O_4$ in acidic solutions would also reduce the number of hydroxyl groups on adsorbent surface, resulting in a decrease in metal adsorption efficiency. The leaching of Co and Fe from adsorbents will be shown and described in the next section.

4.3.4 Leaching of metal from AC-$CoFe_2O_4$

The leaching of metal from AC-$CoFe_2O_4$ composite during adsorption was evaluated by measuring the amount of Co and Fe leaching from solid into the solution with different pH values. The amount of Co and Fe found in solution at different pH were compared to the initial amount in the composite. The sample preparation prior to the determination of the initial Co and Fe amount in the AC-$CoFe_2O_4$ composite by FAAS was adapted from USEPA 3050B method which is the standard method of acid digestion of sediments, sludges and soils. The results are shown in Table 4.2.

Table 4.2 Leaching amount of Co and Fe from the composite during adsorption of Pb(II), Ni(II) and Zn(II) at different pH

Metal pH	Initial amount (mg g^{-1})		Leaching amount (mg g^{-1}) to metal solution					
	Co	Fe	Co			Fe		
			Pb	Ni	Zn	Pb	Ni	Zn
1			24.6	26.9	33.1	46.7	44.3	64.9
2			15.3	15.6	15.7	5.1	3.9	4.8
3	124.2	237.6	12.2	12.5	12.5	0.2	0.1	N.D.
4			10.1	10.9	11.0	0.2	N.D.	N.D.
5			7.3	8.5	9.0	N.D.	N.D.	N.D.
6			3.8	4.5	5.2	N.D.	N.D.	N.D.

N.D. = non detectable

According to the results in Table 4.2, the extent of Co and Fe leaching decreased when increased pH of the metal ion solutions. The leaching of Co and Fe into the metal solutions were in the range of 24.6-33.1 and 46.7-64.9 mg g^{-1} adsorbent at pH 1, respectively. Furthermore, the percentage of leaching of Co and Fe are less than 10% and 1% at pH 4, respectively (see appendix Table C2). The leaching of Co and Fe at pH 1-3 probably caused the low efficiency in removal of metal ions by the adsorbent as shown in previous section. Therefore, this composite is not suitable to use at very low pH.

4.3.5 Adsorption kinetics and effect of adsorbent dosage

Kinetics of adsorption is described in term of the rate of solute adsorbed by the adsorbent. The adsorption kinetics models that are widely used are pseudo-first order model and pseudo-second order model [48-49].

The pseudo-first order equation is generally expressed as shown in equation 4.2,

$$\frac{dq_t}{dt} = k_1(q_e - q_t) \qquad (4.2)$$

where q_e and q_t are the amount of analytes adsorbed on adsorbent at equilibrium and at time t, respectively (mg g^{-1}) and k_1 is the rate constant of pseudo-first order

adsorption (min^{-1}). After integration and applying boundary condition (t = 0 to t = t and q_t = 0 to q_t = q_t), the integration form of equation 4.2 is expressed in equation 4.3.

$$\log(q_e - q_t) = \log q_e - k_1 t \qquad (4.3)$$

The plot between $\log(q_e - q_t)$ and t will give a linear relationship and k_1 and q_e can be determined from the slope and intercept of the linear plot respectively.

The pseudo-second order equation is generally expressed in equation 4.4, where q_e and q_t are the amount of analytes adsorbed on adsorbent at equilibrium and at time t, respectively (mg g^{-1}) and k_2 is the rate constant of pseudo-second order sorption (g mg^{-1} min^{-1}).

$$\frac{dq_t}{dt} = k_2(q_e - q_t)^2 \qquad (4.4)$$

After integration and applying boundary condition (t = 0 to t = t and q_t = 0 to q_t = q_t), the integration form of equation 4.4 is expressed in equation 4.5.

$$\frac{1}{q_e - q_t} = \frac{1}{q_e} + k_2 t \qquad (4.5)$$

Equation 4.5 can be rearranged to equation 4.6.

$$\frac{t}{q_t} = \left(\frac{1}{k_2 q_e^2}\right) + \frac{t}{q_e} \qquad (4.6)$$

The plot between $\dfrac{t}{q_t}$ and t yields a linear line and k_2 and q_e can be determined from the intercept and slope of the graph respectively.

In this experiment, adsorption kinetics and effect of adsorbent dose on adsorption kinetics were studied. The adsorbent dose and adsorption time were varied from 0.01 g to 0.04 g and 5 to 120 min, respectively. The plot of adsorbed amount of metal ions on adsorbent against time, pseudo-first order and pseudo- second order kinetics plot for adsorption of each metal ion on AC-CoFe$_2$O$_4$ are shown in Figure 4.10-4.12.
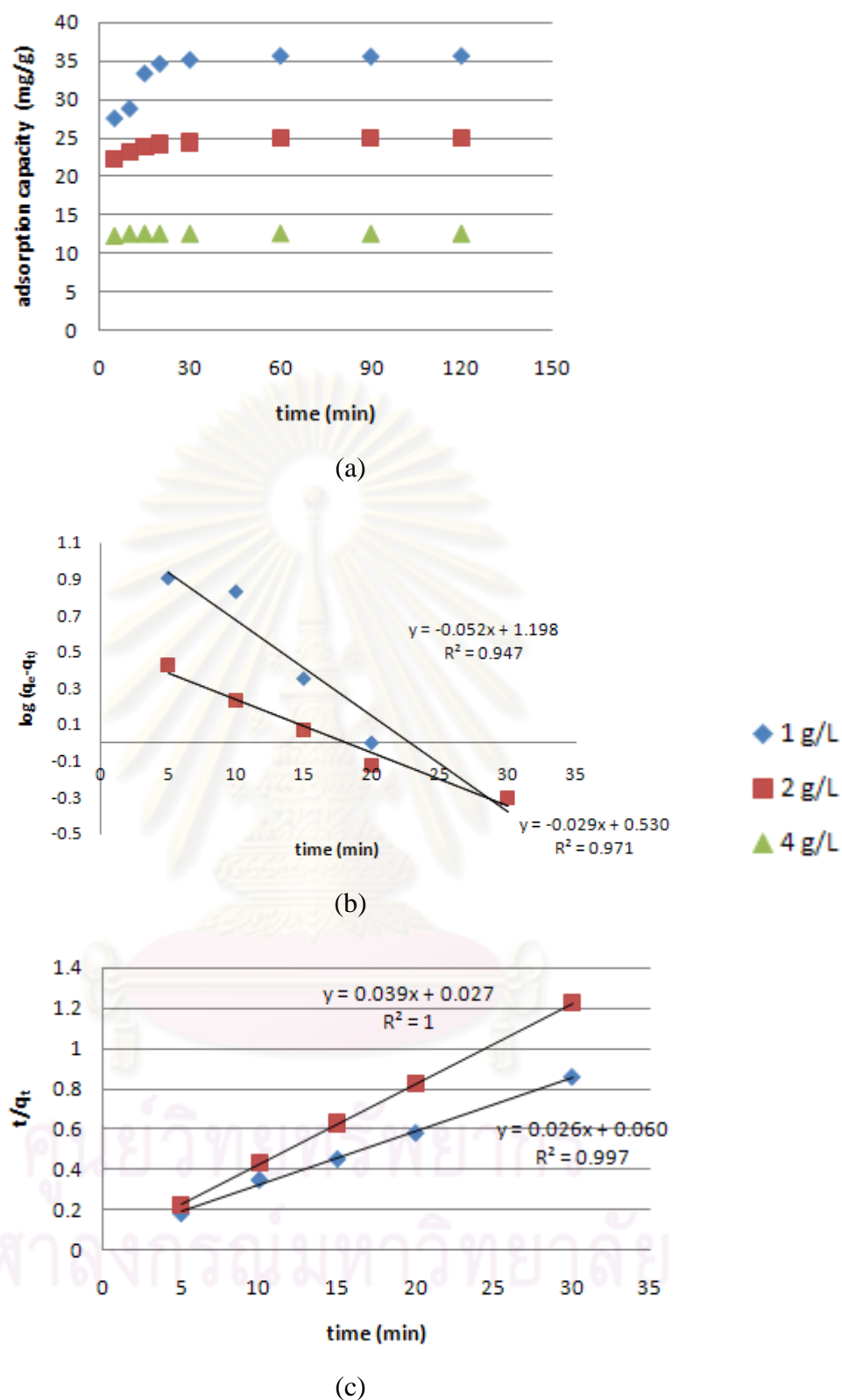
Figure 4.10 The plot of (a) Pb(II) adsorption kinetics, (b) pseudo-first order kinetics model and (c) pseudo- second order kinetics model for adsorption of Pb(II) (50 mg L^{-1}) on AC-CoFe$_2$O$_4$.
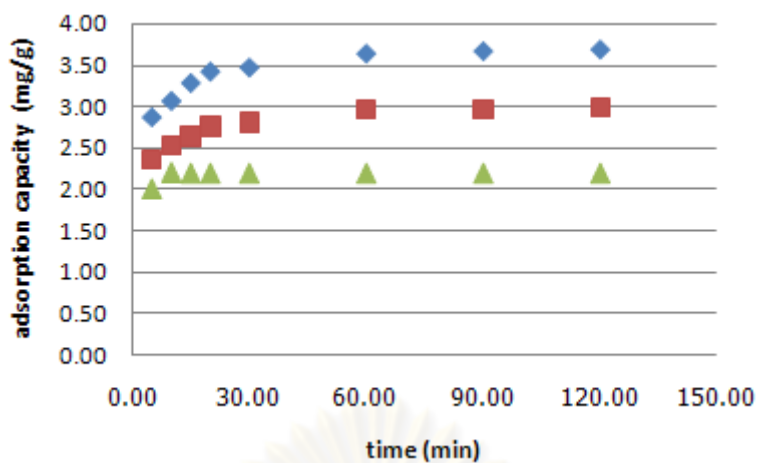
(a)
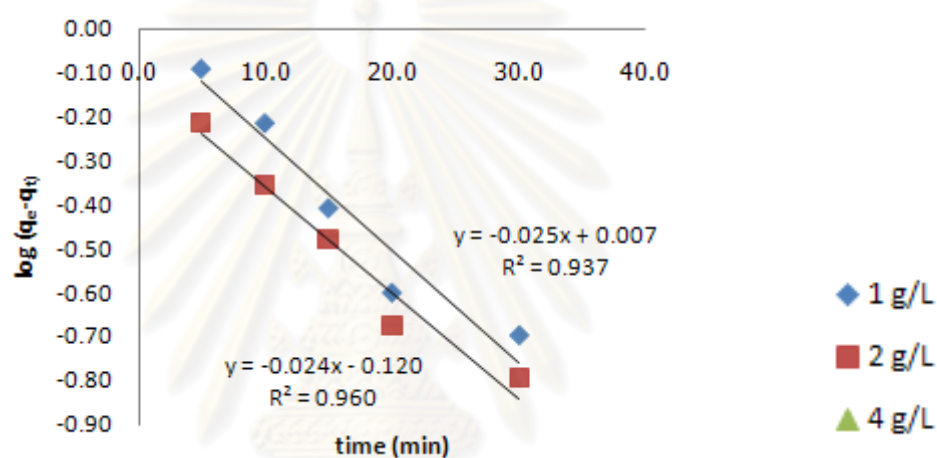
(b)
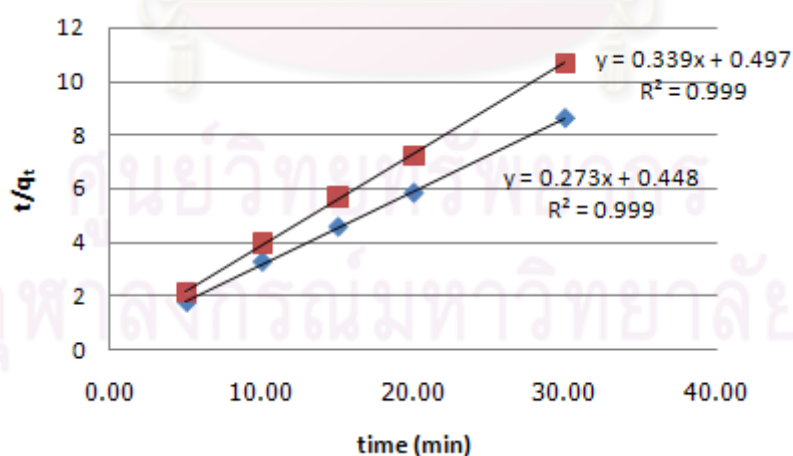
(c)

Figure 4.11 The plot of (a) Ni(II) adsorption kinetics, (b) pseudo-first order kinetics model and (c) pseudo- second order kinetics model for adsorption of Ni(II) (10 mg L^{-1}) on AC-CoFe$_2$O$_4$.

(a)

(b)

(c)
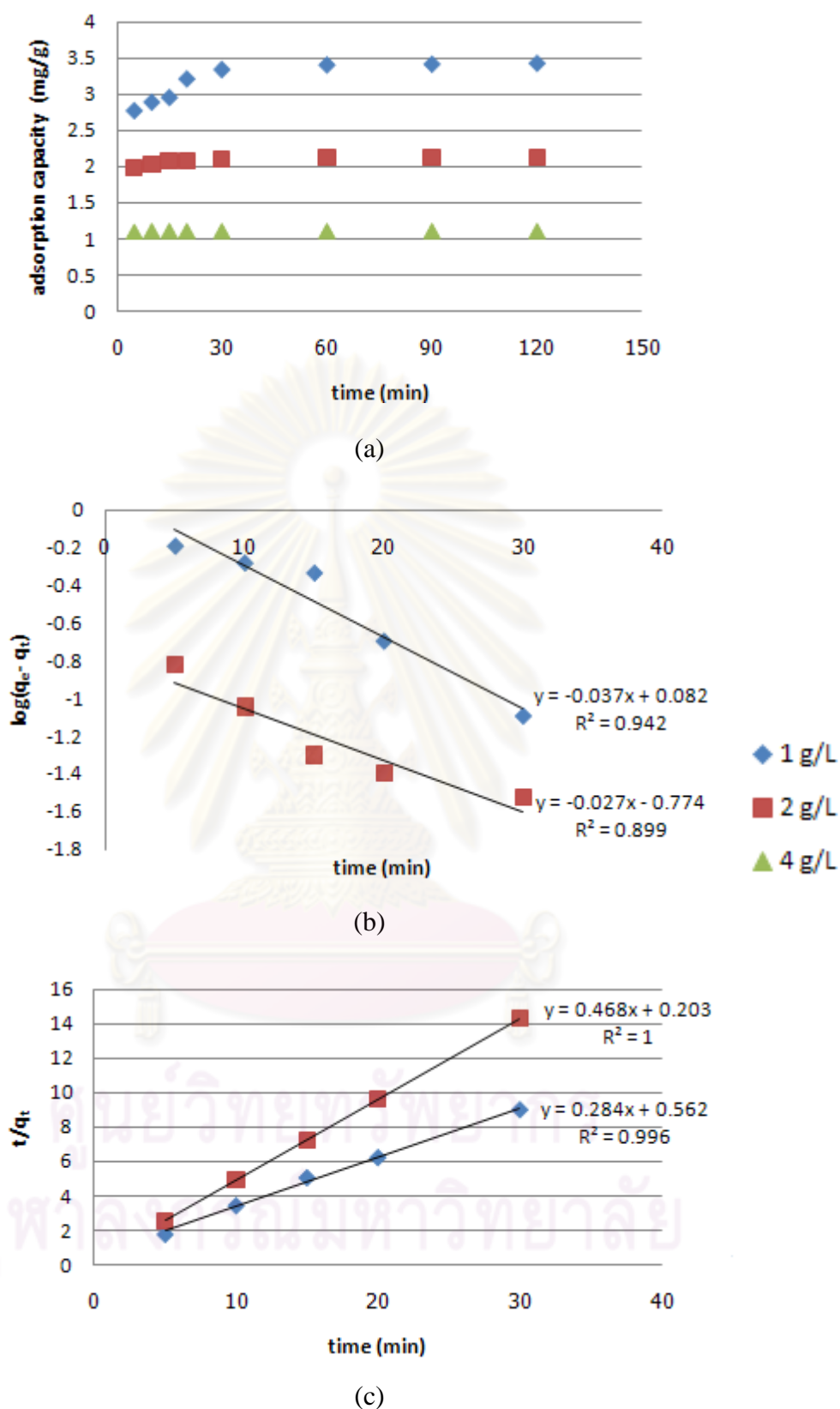
Figure 4.12 The plot of (a) Zn(II) adsorption kinetics, (b) pseudo-first order kinetics
model and (c) pseudo- second order kinetics model for adsorption of
Zn(II) (5 mg L^{-1})on AC-CoFe$_2$O$_4$.

The effect of adsorbent dosage on removal of Pb(II), Ni(II) and Zn(II) ions were studied by varying the amount of adsorbent as 0.01, 0.02 or 0.04 g in 10 mL metal ion solution. The results are shown in Figure 4.10(a), 4.11(a) and 4.12(a). The adsorption capacity of all metal ions (mg g^{-1} adsorbent) decreased with increasing dose. This result can be described by the fact that the adsorbent of higher doses provide more surface area and greater number of active sites for metal ion adsorption. It is basically due to adsorption sites that remained unoccupied during the adsorption process when using high dosage.

Furthermore, the experimental data were fitted to pseudo-first order and pseudo-second order model. The results are summarized in Table 4.3.

Table 4.3 Parameters calculated from pseudo-first order kinetics and pseudo-second order kinetics plot of adsorption of Pb(II), Ni(II) and Zn(II) ions on AC-CoFe$_2$O$_4$

| Kinetics model | Metal | Adsorbent dose (g) | $q_{e,\exp}$ (mg g^{-1}) | $q_{e,cal}$ (mg g^{-1}) | Kinetic constant | | r^2 |
					k_1 (min^{-1})	k_2 (g mg^{-1} min^{-1})	
Pseudo-first order	Pb	0.0100	35.58	15.78	0.052		0.947
		0.0200	25.00	3.39	0.029		0.971
	Ni	0.0100	3.67	1.02	0.025		0.937
		0.0200	2.97	0.76	0.024		0.960
	Zn	0.0100	3.41	1.21	0.037		0.942
		0.0200	2.13	5.94	0.027		0.899
Pseudo-second order	Pb	0.0100	35.58	38.46		0.011	0.997
		0.0200	25.00	25.64		0.056	1.000
	Ni	0.0100	3.67	3.66		0.167	0.999
		0.0200	2.97	2.95		0.231	0.999
	Zn	0.0100	3.41	3.52		0.144	1.000
		0.0200	2.13	2.14		1.079	0.996

$q_{e,\exp}$ represents the adsorption capacity at equilibrium from the experiment.

$q_{e,cal}$ represents the adsorption capacity at equilibrium calculated from the linear equation of kinetics model plots.

The results show that the adsorption data of all metal ions could fit well to the pseudo-second order model as demonstrated by the r^2 values that were higher than the values from the linear fit to the pseudo-first order model. Moreover, the calculated adsorption capacities at equilibrium ($q_{e,cal}$) obtained from the pseudo-second order plot are closer to the experimental data ($q_{e,\exp}$) than $q_{e,cal}$ obtained from the pseudo-first order linear plot. Therefore, the kinetics of all metal ions adsorption on AC-CoFe$_2$O$_4$ followed the pseudo-second order model. The second order rate constants (k$_2$) increase when the dose increases, indicating that the adsorption reaches the adsorption equilibrium in shorter time when using higher dose.

As shown in Figure 4.10(a), 4.11(a) and 4.12(a), it can be seen that the adsorption equilibrium was reached rapidly when used the dosage of 4 g L^{-1} for all metal ions, so there was not enough the data point to fit either pseudo-first order and pseudo-second order model.

The results from kinetics study indicate that the adsorption of metal ions on AC-CoFe$_2$O$_4$ followed the assumptions of the pseudo-second order model that are [49-50],

- The metal ions adsorption occurred as monolayer sorption.
- The energy of the metal ions adsorption is unique.
- There is no interaction between adsorbed metal ions.
- The rate of adsorption can be neglected compared with the initial rate of adsorption.

4.3.6 Adsorption isotherms

The adsorption equilibrium between metal ions in aqueous phase and the AC-CoFe$_2$O$_4$ phase can be described by adsorption isotherm. Several isotherm equations are available but only two important isotherm models i.e. Langmuir isotherm and Freundlich isotherm are widely used. Langmuir adsorption isotherm assumes monolayer adsorption on homogeneous surface with a specific number of adsorption sites. The equation is shown in equation 4.7 [51],

$$\frac{C_e}{q} = \frac{1}{bq_m} + \frac{C_e}{q_m} \qquad (4.7)$$

where q =   the amount of metal ions adsorbed per weight of adsorbent at equilibrium (mg g^{-1})

       C_e =   the equilibrium concentration of the metal ions in solution (mg L^{-1})

       q_m =   the maximum adsorption capacity (mg g^{-1})

       b =   the constant related to the free energy of adsorption (L mg^{-1})

Freundlich adsorption isotherm assumes that the uptake of metal ions occurs on a heterogeneous surface in multilayer regime. The Freundlich isotherm is expressed in equation 4.8 [52],

$$\log q = \log K_f + \frac{1}{n}\log C_e \qquad (4.8)$$

where K_f =   a constant indicative of the relative adsorption capacity of the adsorbent (mg g^{-1})

       n =   a constant related to the intensity of the adsorption

The adsorption isotherm experiments were carried out at initial pH 5 for Pb(II) and 6 for Ni(II) and Zn(II) by varying the initial concentration of these metal ions in the range of 1 to 400 mg L^{-1} at 28°C. The plots of equilibrium concentration of metal ions in solution against adsorption capacity of AC-CoFe$_2$O$_4$ are presented in Figure 4.13.
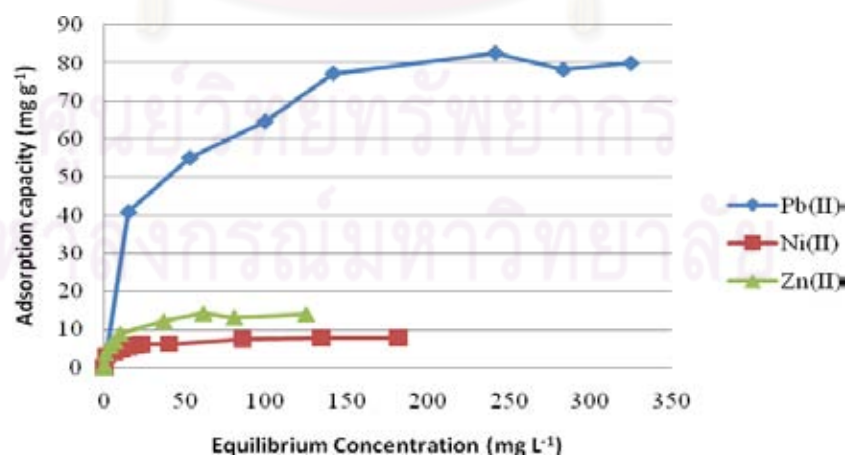
Figure 4.13 The relation between concentration at equilibrium of metal ions and adsorption capacity of AC-CoFe$_2$O$_4$.

The experimental data were used in the linear plot of Langmuir equation ($\frac{C_e}{q}$ versus C_e) and Freundlich equation ($\log q$ versus $\log C_e$) and the results are shown in Figure 4.14 and 4.15, respectively.
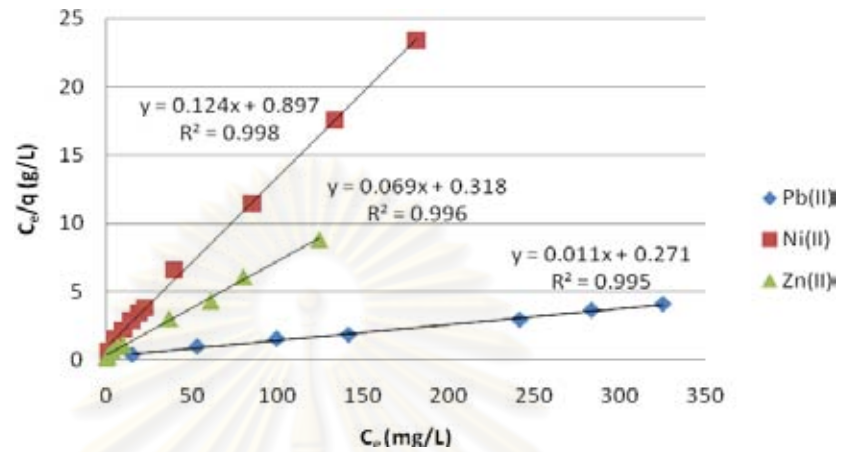
Figure 4.14 Langmuir isotherm plot for the adsorption of Pb(II), Ni(II) and Zn(II) ions on AC-CoFe$_2$O$_4$.
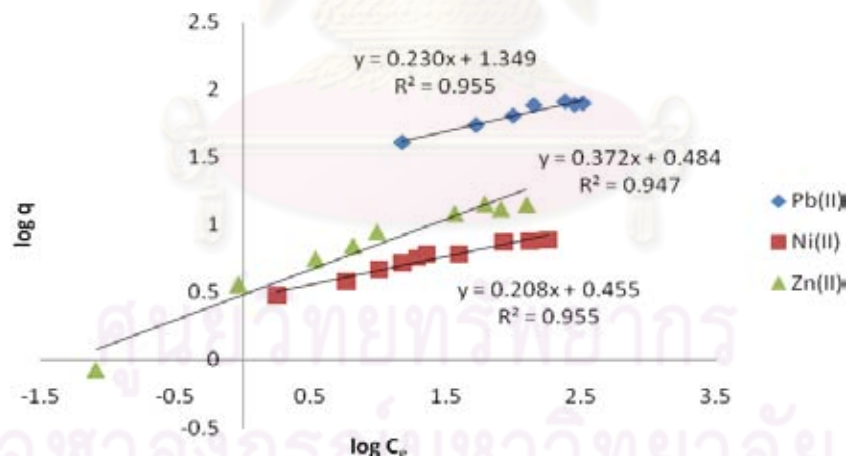
Figure4.15 Freundlich isotherm plot for the adsorption of Pb(II), Ni(II) and Zn(II) ions on AC-CoFe$_2$O$_4$.

By fitting the experimental data to the isotherm model, the Langmuir and Freundlich constants could be determined as listed in Table 4.4.

Table 4.4 Langmuir and Freundlich constants for adsorption of metal ions on AC-
    $CoFe_2O_4$

Metal	Langmuir constants				Freundlich constants		
	q_m (mg g^{-1})	b (L mg^{-1})	r^2	R_L	K_f (mg g^{-1})	n	r^2
Pb(II)	90.91	0.040	0.995	0.058-0.309	22.32	0.23	0.955
Ni(II)	8.06	0.138	0.998	0.037-0.602	2.85	0.21	0.955
Zn(II)	14.49	0.217	0.996	0.032-0.832	3.05	0.37	0.947

As shown in Table 4.4, the experimental data were better fit by Langmuir model than Freundlich model for all metal ions. All of the r^2 values from Langmuir fitting were higher than 0.99. The results lead to an assumption that the adsorption of metal ions on adsorbent occurred as monolayer adsorption without interaction between adsorbed molecules. This result was confirmed by the result from kinetics study that the adsorption kinetics followed pseudo-second order model (Section 4.3.5) which was derived based on the monolayer adsorption assumption.

This result shows that the adsorption of metal ions onto the AC-$CoFe_2O_4$ followed the Langmuir adsorption isotherm model which assumed the adsorption on homogeneous surface active site. In the composite, there are two components including activated carbon and $CoFe_2O_4$ and it contained heterogeneous surface active sites. However, the result from the topic 4.3.1 showed that the activated carbon itself had very low efficiency in metal ions adsorption. Therefore, the major active sites on the composite AC-$CoFe_2O_4$ that are responsible to the metal ions adsorption was those of $CoFe_2O_4$.

In addition, the essential characteristics of Langmuir isotherm that explain whether the adsorption system is favorable or unfavorable is R_L parameter, calculated by equation 4.9,

$$R_L = \frac{1}{1 + bC_i} \qquad (4.9)$$

where b = the constant related to the free energy of adsorption (L mg^{-1})

C_i = initial concentration of metal ions (mg L^{-1})

The parameter R_L indicates the type of isotherm as presented in Table 4.5.

Table 4.5 R_L value that associates with the type of isotherm

Value of R_L	Type of isotherm
$R_L > 1$	Unfavorable
$R_L = 1$	Linear
$0 < R_L < 1$	Favorable
$R_L = 0$	Irreversible

The values of R_L were calculated from the data as shown in Table 4.4 and compared to the values given in Table 4.5. The results indicate that the adsorption of Pb(II), Ni(II) and Zn(II) is favorable. The maximum adsorption capacity were 90.91, 8.06 and 14.49 mg g^{-1} for adsorption of Pb(II),Ni(II) and Zn(II) ions onto AC-CoFe$_2$O$_4$, respectively.

The maximum capacity of AC-CoFe$_2$O$_4$ and other adsorbents in metal ions adsorption are compared in Table 4.6.

Table 4.6 Adsorption capacity of some adsorbents for removal of Pb(II), Ni(II) and Zn(II)

Type of adsorbent	Metal adsorption capacity of adsorbents (mmol g^{-1})	Reference
AC-CoFe$_2$O$_4$	Pb(II) (0.439), Ni(II) (0.137), Zn(II) (0.222)	this work
Manganese dioxide-iron oxide magnetic composite	Pb(II) (2.18), Ni(II) (0.601)	[36]
Zeolite-iron oxide magnetic composite	Zn(II) (1.7)	[38]

Table 4.6 (continued)

Type of adsorbent	Metal adsorption capacity of adsorbents (mmol g^{-1})	Reference
Zeolite-iron oxide magnetic composite	Pb(II) (0.59)	[39]
Tea waste impregnated with iron oxide	Ni(II) (0.65)	[40]
Multiwall carbon nanotube/ iron oxide magnetic composite	Ni(II) (0.16)	[41]
Iron oxide coated waste silica gel	Pb(II) (0.039), Ni(II) (0.072)	[53]
Amino functionalized iron oxide-silica	Pb(II) (0.54)	[54]
Iron oxide modified sewage sludge	Pb(II) (0.20), Ni(II) (0.13)	[55]

The results show that the adsorbent prepared in this work has moderate efficiency for removal of Pb(II), Ni(II) and Zn(II), compared to different types of magnetic adsorbents and adsorbents containing iron oxide.

4.3.7 Effect of salt

The presence of ions other than studied metal ions may affect the adsorption efficiency of AC-CoFe$_2$O$_4$ toward target metal ions. To evaluate the affect of salts on the adsorption of metal ions, the adsorption of metal ions were performed in the presence of NaNO$_3$, Na$_2$SO$_4$ and Ca(NO$_3$)$_2$ which are often found in large

amount in battery industry wastewater. These salts were added to the metal ions solution with the concentration of 0.1 or 1.0 M. The results are shown in Figure 4.16.
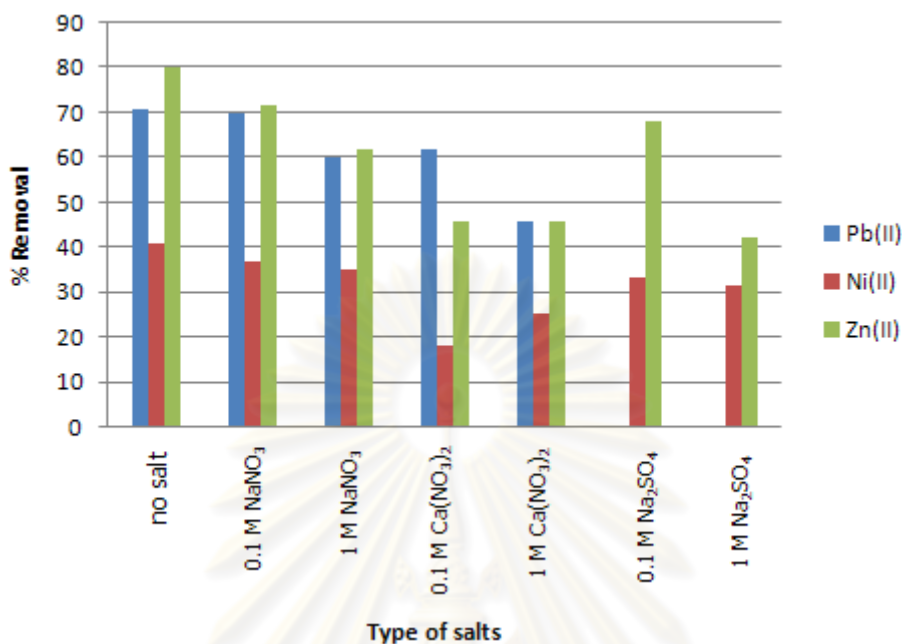
Figure 4.16 Effect of salts on the removal of Pb(II), Ni(II) and Zn(II) ions by
AC-CoFe$_2$O$_4$.

There was no results of the effect of Na$_2$SO$_4$ on Pb(II) adsorption because of the precipitation of PbSO$_4$. The presence of salts affected the removal of metal ions by AC-CoFe$_2$O$_4$. The adsorption efficiency decreased by increasing the salt concentration.

In the presence of salts, the ionic strength of the solution was changed resulting in the change in metal adsorption at equilibrium. It was observed that when increasing concentration of salt or when the ionic strength of solution increased, the efficiency in removal of all metal ions by the adsorbent decreased. For example, the removal efficiency achieved in solution containing 1 M NaNO$_3$ was higher than in solution containing 1 M Na$_2$SO$_4$, which had higher ionic strength.

4.4 Application in treatment of wastewater sample from battery factory

In this work, the wastewater from a battery factory was collected, analyzed and used in the experiment for metal ions removal. The wastewater was filtered and

the pH of the sample was measured. Then, the sample was analyzed by ICP-OES. The metal ions found in wastewater included Cu, Cd, Fe, Pb, Ni, Zn and Ca.

Furthermore, the pH of the sample was 1.42 which was very low and would result in the dissolution of $CoFe_2O_4$ on the adsorbent if used the adsorbent at this pH. Therefore, the pH of the sample was risen up to pH 6. A brown precipitate occurred during pH adjustment and was separated from wastewater prior to adsorption experiment. The concentrations of metals before and after pH adjustment were determined by FAAS and ICP-OES. The results are shown in Table 4.7.

Table 4.7 The concentration of transition metal ions in wastewater before and after pH adjustment and concentration after adsorption by AC-CoFe$_2$O$_4$ and percentage of removal

Metal	Concentration (mg L^{-1})			%Removal[c]
	Before pH adjustment[a]	After pH adjustment	After adsorption by AC-CoFe$_2$O$_4$	
Fe	497.78 ± 3.85	0.86 ± 0.03[b]	0.28 ± 0.13[b]	67.44
Cd	8.52 ± 0.00	2.63 ± 0.09[b]	2.36 ± 0.11[b]	10.27
Cu	4.10 ± 0.02	0.48 ± 0.05[b]	0.02 ± 0.01[b]	95.83
Pb	3.64 ± 0.10	0.04 ± 0.01[b]	0.03 ± 0.00[b]	25.00
Ni	1.87 ± 0.02	1.43 ± 0.03[a]	1.28 ± 0.04[a]	10.49
Zn	13.74 ± 0.18	11.44 ± 0.15[a]	7.26 ± 0.21[a]	36.54

Ca^{2+} concentration measured by FAES after pH adjustment was 480.53±2.79 mg L^{-1}.

Mean ± S.D. (N=3)

[a] measured by FAAS

[b] measured by ICP-OES

[c] calculated from the residual metal concentration after adsorption against the concentration of metal in sample after pH adjustment

The major transition metal in the wastewater was iron and the solution of the wastewater before pH adjustment was pale yellow. Regarding the K_{sp} value [56] of iron(II) and iron (III) hydroxide that are very low (8×10^{-16} and 4×10^{-38}, respectively), iron would precipitate when increased the solution pH. A brown precipitate was also obtained during pH adjustment. When the iron precipitated, it

would induce other metal ions to co-precipitate or other metal ions would adsorb on ferric hydroxide floc, resulting in the reduction of the concentration of other metals in the wastewater.

From Table 4.7, the removal efficiency of AC-CoFe$_2$O$_4$ toward studied metals is low. The adsorbed amount of metals on the adsorbent were 0.01, 0.15 and 4.18 mg Pb(II), Ni(II) and Zn(II) per gram adsorbent, respectively, which were very low when compared with the maximum adsorption capacity of the adsorbents for these metal ions. It can be explained by the presence of other transition metal ions and also other salts such as Ca^{2+} salt that compete with the target metal ions in adsorption onto adsorbent.

In conclusion, the application of this adsorbent in extremely low pH and high concentration of salt is not recommended. It should be used to treatment the contaminated natural water to avoid the salt effect.

CHAPTER V

CONCLUSION

The composite of activated carbon and $CoFe_2O_4$ was successfully synthesized by co-precipitation method. The obtained $AC\text{-}CoFe_2O_4$ has better dispersion ability in water than $CoFe_2O_4$. The $AC\text{-}CoFe_2O_4$ was characterized by X-ray diffraction, fourier transform infrared spectroscopy, surface area analysis and scanning electron microscope. The results from all characterization techniques confirmed that the composite of activated carbon and $CoFe_2O_4$ was obtained.

The $AC\text{-}CoFe_2O_4$ showed higher efficiency in metal ions adsorption than activated carbon and $CoFe_2O_4$. The suitable condition for removal of Pb(II), Ni(II) and Zn(II) from solutions by $AC\text{-}CoFe_2O_4$ were studied using batch system. The adsorption equilibrium could be attained after 60 min of contact time for Pb(II) and Ni(II) and after 120 min for Zn(II). The removal of all metal ions increased obviously with an increasing of solution pH and the suitable pH values for metal ions extraction were pH 6. When the pH of solution was low (1-3), there were leaching of Co and Fe from the adsorbent.

The removal efficiency of all metal ions was improved with increasing adsorbent dose from 1 g L^{-1} to 4 g L^{-1}. The adsorption kinetics followed the pseudo-second order kinetics for $AC\text{-}CoFe_2O_4$ and the rate of adsorption increased with increasing of adsorbent dosage at constant temperature.

From adsorption isotherm studies, the results showed that the adsorption of Pb(II), Ni(II) and Zn(II) ions on $AC\text{-}CoFe_2O_4$ fit the Langmuir adsorption isotherm model better than Freundlich model. Under the assumption of Langmuir model, the uptake of metal ions occurred as monolayer sorption without interaction between sorbed molecules. The maximum adsorption capacity of the adsorbent for Pb(II), Ni(II) and Zn(II) were 90.91, 8.06 and 14.49 mg g^{-1}, respectively.

Furthermore, the presence of salts including sodium nitrate, sodium sulfate and calcium nitrate at 0.1 M and 1.0 M obviously reduced the metal ions removal efficiency of $AC\text{-}CoFe_2O_4$. Finally, the use of material in extreme condition as low pH and high concentration of salt is not recommended.

Suggestions for future work

- The reusability of AC-CoFe$_2$O$_4$ should be studied.
- The composite can be modified with functional group to protect the surface for adsorption at low pH and to improve the selectivity toward the metal ions.

REFERENCES

[1] Sharma, S.K., Sehkon, N.S., Deswal, S., and John, S. Transport and fate of copper in soils. J. Civil. Environ. Eng. (2009) [Online] Avialable from : http://www.waset.org/journals/ijcee/v1/v1-1-1.pdf [2010, November 22]

[2] Zhou, P., Huang, J.C., Li, A.W.F. and Wei, S. Heavy metal removal from wastewater in fluidized bed reactor. Wat. Res. 33 (1999): 1918-1924.

[3] Afkhami, A., Tehrani, M.S., and Bagheri, H. Simultaneous removal of heavy-metal ions in wastewater samples using nano-alumina modified with 2,4-dinitrophenylhydrazine. J. Hazard. Mater. 181 (2010): 836-844.

[4] Blöcher C., et al. Hybrid flotation-membrane filtration process for the removal of heavy metal ions from wastewater Wat. Res. 37 (2003): 4018-4026.

[5] Juang, R.S., and Wang, S.W. Electrolytic recovery of binary metals and EDTA form strong complexed solutions. Wat. Res. 34 (2000): 3179-3185.

[6] Belkhouche, N.E., Didi, M.A., Romero, R., Jönsson, J.A., and Villemin, D. Study of new organophosphorus derivates carriers on the selective recovery of M(II) and M(III) metals, using supported liquid membrane extraction. J. Mem. Sci. 284 (2006): 398-405.

[7] Dong, J., Xu, Z., and Wang, F. Engineering and characterization of mesoporous silica-coated magnetic particles for mercury removal from industrial effluents. App. Surf. Sci. 254 (2008): 3522-3530.

[8] Nacev, A., Beni, C., Bruno, O., and Shapiro, B. The behaviors of ferromagnetic nano-particles in and around blood vessels under applied magnetic fields. J. Magn. Magn. Mat. 323 (2011): 651-668.

[9] Avilés, M.O., Ebner, A.D., and Ritter, J.A. In vitro study of magnetic particle seeding for implant-assisted-magnetic drug targeting: Seed and magnetic drug carrier particle capture. J. Magn. Magn. Mat. 321 (2009): 1586-1590.

[10] Feng, Y., and others. Adsorption of Cd(II) and Zn(II) from aqueous solutions using magnetic hydroxyapatite nanoparticles as adsorbents. J. Chem. Eng. 162 (2010): 487-494.

[11] Lin, Y.F., Chen, H.W., Chien, P.S., Chiou, C.S., and Liu, C.C. Application of bifunctional magnetic adsorbent to adsorb metal cations and anionic dyes in aqueous solution. J. Harzard. Mater. 185 (2011): 1124-1130.

[12] Laska, U., Frost, C.G., Price, G.J., and Plucinski, P.K. Easy-separable magnetic nanoparticle-supported Pd catalysts: Kinetics, Stability and catalyst re-use. J. cat. 268 (2009): 318-328.

[13] Pramanik, N.C., Fujii, T., Nakanishi, M., and Takada, J. Effect of Co^{2+} ion on the magnetic properties of sol-gel cobalt ferrite thin films. J. Mat. Chem. 14 (2004): 3328-3332.

[14] Lung, C.H., Hsiung, L.K., Yu, C.S., Guan, C.C., and De, P.S. Dye adsorption on biosolid adsorbents and commercially activated carbon. Dyes Pigments. 75 (2007): 52-59.

[15] Rao, M.M., Ramana, D.K., Seshaiah, K., Wang, M.C., and Chien, S.W.C. Removal of some metal ions by activated carbon prepared from Phaseolus aureus hulls. J. Hazard. Mat. 166 (2009): 1006-1013.

[16] Monser, L., and Adhoum, N. Tartrazine modified activated carbon for removal of Pb(II), Cd(II) and Cr(III). J. Hazard. Mater. 161 (2009): 263-269.

[17] Zhu, L., and others. Mixed hemimicelles SPE based on CTAB coated Fe_3O_4/SiO_2 NPs for the determination of herbal bioactive constituents from biological samples. Talanta 80 (2010): 1873-1880.

[18] Magnetic materials [Online]. Science and Technology knowledge center. Available from : http://www1.stkc.go.th/content.php?url=stportal Document/1185724013.html [2010, December 8]

[19] Mathew, D.S., and Juang, R.S. An overview of the structure and magnetism of spinel ferrite nanoparticles and their synthesis in microemulsions. J. Chem. Eng. 129 (2007): 51-65.

[20] Crystal structure of cubic spinel [Online]. Knol. Available from : http://knol.google.com/k/spinel-oxides# [2011, January 6]

[21] Crystal structure of CoFe$_2$O$_4$ [Online]. Wikimedia Foundation. Available from : http://wikis.lib.ncsu.edu/index.php/Spinel [2011, January 6]

[22] Meron, T., Rosenberg, Y., Lereah, Y., and Markovich, G. Synthesis and assembly of high-quality cobalt ferrite nanocrystal prepared by a modified sol-gel technique. J. Magn. Magn. Mat. 292 (2005): 11-16.

[23] Akl, J., Ghaddar, T., Ghanem, A., and Rassy, H.E. Cobalt ferrite aerogels by epoxide sol-gel addition: Efficient catalysts for the hydrolysis of 4-nitrophenyl phosphate. J. Mol. Cat. A 312 (2009): 18-22.

[24] Gul, I.H., Maqsood, A., Naeem, M., and Ashiq, M.N. Optical, magnetic and electrical investigation of cobalt ferrite nanoparticles synthesized by co-precipitaion route. J. Alloys Compd. 507 (2010): 201-206.

[25] Khandekar, M.S., Kambale, R.C., Patil, J.Y., Kolekar, Y.D., and Suryavanshi, S.S. Effect of calcinations temperature on the structural and electrical properties of cobalt ferrite synthesized by combustion method. J. Alloys Compd. 509 (2011): 1861-1865.

[26] Marsh, H., and Reinoso, F.R. Activated carbon, 1st ed., Elsevier Academic Press, Inc., (2006): 1

[27] Ahn, C.K., Park, D., Woo, S.H., and Park, J.M. Removal of cationic heavy metal from aqueous solution by activated carbon impregnated with anionic surfactant. J. Hazard. Mater. 164 (2009): 1130-1136.

[28] Information of lead [Online]. Thiland junior encyclopedia project. Available from :http://kanchanapisek.or.th/kp6/New/sub/book/book.php?book=22& chap=6&page=t22-6-infodetail01.html [2011, January 19]

[29] Information of nickel [Online]. Wikimedia Foundation. Available from : http://en.wikipedia.org/wiki/Nickel [2011, January 19]

[30] Information of zinc [Online]. Wikimedia Foundation. Available from : http://en.wikipedia.org/wiki/Zinc [2011, January 19]

[31] Fu, F., and Wang, Q. Removal of heavy metal ions from wastewaters : A review. J. Environ. Manage. 92 (2011) 407-418.

[32] Bradl, H.R. Heavy metals in the environment. New York, USA. : Elsevier Academic Press, Inc., (2005).

[33] Vithaya Ruangpornvisuti. Catalysis surface chemistry and petrochemical., Thailand. 1st ed. Technology Promotion Association (Thailand-Japan) Publication: (2004).

[34] Hamdaoui, O., and Naffrechoux, E. Modeling of adsorption isotherms of phenols and chlorophenols onto granular activated carbon Part I. two-parameter models and equations allowing determination of thermodynamic parameters. J. Hazard. Mat. 147 (2007): 381-394.

[35] Goldberg, S., Criscenti, L.J., Turner, D.R., Davis, J.A., and Cantrell, K.J. Adsorption-desorption process in subsurface reactive transport modeling. Vandose Zone J. 6 (2007): 407-435.

[36] Rosas, C.A.C., Franzreb, M., Valenzuela, F., and Höll, W.H. Magnetic manganese dioxide as an amphoteric adsorbent for removal of harmful inorganic contaminants from water. React. Funct. Polym. 70 (2010): 516-520.

[37] Wei, L., Yang, G., Wang, R., and Ma, W. Selective adsorption and separation of chromium(VI) on the magnetic iron-nickel oxide from waste nickel liquid. J. Hazard. Mater. 164 (2009): 1159-1163.

[38] Oliveira, L.C.A., Petkowicz, D.I., Smaniotto, A., and Pergher, S.B.C. Magnetic zeolites: a new adsorbent for removal of metallic contaminants from water. Wat. Res. 38 (2004): 3699-3704.

[39] Nah, I.W., Hwang, K.Y., Jeon, C., and Choi, H.B. Removal of Pb ion from water by magnetically modified zeolite. Min. Eng. 19 (2006): 1452-1455.

[40] Panneerselvam, P., Morad, N., and Tan, K.A. Magnetic nanoparticle (Fe_3O_4) impregnated onto tea waste for the removal of nickel(II) from aqueous solution. J. Harzard Meter. 186 (2011): 160-168.

[41] Chen, C., Hu, J., Shao, D., Li, J., and Wang, X. Adsorption behavior of multiwall carbon nanotube/iron oxide magnetic composites for Ni(II) and Sr(II). J. Hazard. Mater. 164 (2009): 923-928.

[42] Ai, L., Huang, H., Chen, Z., Wei, X., and Jiang, J. Activated carbon/$CoFe_2O_4$ composites: Facile synthesis, magnetic performance and their potential application for the removal of malachite green from water. J. Chem. Eng. 156 (2010): 243-249.

[43] Method 3050B. Acid digestion of sediments, sludges and soils. USEPA. 1996.

[44] Wade, L.G. Organic chemistry. 6th ed. Pearson Education Inc. (2004).

[45] Liu, Z., Zhang, F.S. and Sasai, R. Arsenate removal from water using Fe_3O_4-loaded activated carbon prepared from waste biomass. J. Chem. Eng. 160 (2010): 57-62.

[46] Tourinho, F.A., Franck, R., and Massart, R. Aqueous ferrofluids based on manganese and cobalt ferrite. J. Mater. Sci. 25 (1990): 3249-3254.

[47] Dzombak, D.A., and Morel, F.M.M. Surface Complexation Modeling, Hydrous Ferric Oxide. John Wiley & Sons, Inc. 1990.

[48] Lagergren, S. About the theory of so-called adsorption of soluble substances. Kungliga Svenska Vetenskapsakademiens, Handlingar, Band 24 (1898): 1–39.

[49] Ho, Y.S. and McKay, G., Pseudo-second order model for sorption processes, Process Biochem. 34 (1999): 451–465.

[50] Ofomaja, A.E., Naidoo, E.B., and Modise, S.J. Dynamic studies and pseudo-second order modeling of copper(II) biosorption onto pine cone powder. Desalination. 251 (2010): 112-122.

[51] Langmuir, I. The adsorption of gases on plane surfaces of glass, mica and platinum. J. Am. Chem. Soc. 40 (1918): 1361–1403.

[52] Freundlich H. Über die adsorption in lösungen (Adsorption in solution), Z. Phys. Chem. 57 (1906): 384–470.

[53] Unob, F., Wongsiri, B., Phaeon, N., Puanngam, M., and Shiowatana, J. Reuse of waste silica as adsorbent for metal removal by iron oxide modification. J. Hazard. Meter. 142 (2007): 455-462.

[54] Wang, J., and others. Amino-functionalized $Fe_3O_4@SiO_2$ core-shell magnetic nanomaterial as a novel adsorbent for aqueous heavy metals removal. J. Colloid Interface Sci. 349 (2010): 293-299.

[55] Phuengprasop, T., Sittiwong, J., and Unob, F. Removal of heavy metal ions by iron oxide coated sewage sludge. J. Harzard Meter. 186 (2011): 502-507.

[56] Chaitiamwong, S. Quantitative analysis Chemistry Laboratory Chulalongkorn University Publication, 6 (2000): 247.

APPENDICES

APPENDIX A

Comparison of adsorption efficiency of activated carbon, $CoFe_2O_4$ and $AC\text{-}CoFe_2O_4$

Table A1 Comparison of adsorption efficiency of activated carbon, $CoFe_2O_4$ and $AC\text{-}CoFe_2O_4$

Adsorbents	Adsorbed amount of metal ions ($mg\ g^{-1}$)			% Removal		
	Pb(II)	Ni(II)	Zn(II)	Pb(II)	Ni(II)	Zn(II)
Activated carbon	4.44 ± 0.00	0.49 ± 0.12	0.77 ± 0.25	8.33 ± 0.00	1.74 ± 0.43	5.10 ± 1.67
$CoFe_2O_4$	18.15 ± 2.57	3.82 ± 0.43	5.35 ± 0.38	34.02 ± 4.81	13.68 ± 1.55	35.36 ± 2.53
$AC\text{-}CoFe_2O_4$	29.81 ± 0.32	4.86 ± 0.12	7.34 ± 0.29	55.89 ± 0.60	17.41 ± 0.43	48.48 ± 1.26

Mean $\pm$ S.D. (N=3)

APPENDIX B

Effect of contact time

Table B1   Effect of contact time on the adsorption of Pb(II), Ni(II) and Zn(II) by
using AC-CoFe$_2$O$_4$

Time (min)	Adsorbed amount of metal ions (mg g^{-1})			% Removal		
	Pb(II)	**Ni(II)**	**Zn(II)**	**Pb(II)**	**Ni(II)**	**Zn(II)**
30	21.67 ± 0.83	5.73 ± 0.15	5.84 ± 0.09	44.83 ± 1.72	19.09 ± 0.49	38.56 ± 0.61
60	23.89 ± 0.96[a]	6.07 ± 0.15[a]	6.58 ± 0.09	49.43 ± 1.99	20.23 ± 0.49	43.47 ± 0.61
90	23.89 ± 0.48	6.32 ± 0.15	6.74 ± 0.24	49.43 ± 1.00	21.08 ± 0.49	44.52 ± 1.61
120	23.61 ± 0.48	6.41 ± 0.26	7.32 ± 0.16[a]	48.85 ± 1.00	21.37 ± 0.85	48.38 ± 1.05
180	24.44 ± 1.27	6.50 ± 0.15	7.59 ± 0.09	50.57 ± 2.63	21.65 ± 0.49	50.13 ± 0.61
240	25.00 ± 0.00	6.58 ± 0.15	7.54 ± 0.09	51.72 ± 0.00	21.94 ± 0.49	49.78 ± 0.61

Mean ± S.D. (N=3)

[a] superscript indicate no significant difference of time since marked

Table B2   A statistical test difference contact time (30 – 240 min) of Pb(II) by
using one-way ANOVA at significant = 0.01

Source of variation	SS	df	MS	F	F$_{cririca l}$
Between time	82.72	5	16.54	6.27	5.06
With in time	31.64	12	2.64		
total	114.36	17			

Table B3   A statistical test difference contact time (60 – 240 min) of Pb(II) by
using one-way ANOVA at significant = 0.01

Source of variation	SS	df	MS	F	F$_{cririca l}$
Between time	15.79	4	3.95	1.54	5.99
With in time	25.70	10	2.57		
total	41.49	14			

Table B4   A statistical test difference contact time (30 – 240 min) of Ni(II) by
using one-way ANOVA at significant = 0.01

Source of variation	SS	df	MS	F	$F_{cririca l}$
Between time	16.90	5	3.38	10.40	5.06
With in time	3.90	12	0.33		
total	20.80	17			

Table B5   A statistical test difference contact time (60 – 240 min) of Ni(II) by
using one-way ANOVA at significant = 0.01

Source of variation	SS	df	MS	F	$F_{cririca l}$
Between time	5.17	4	1.29	3.80	5.99
With in time	3.40	10	0.34		
total	8.57	14			

Table B6   A statistical test difference contact time (30 – 240 min) of Zn(II) by
using one-way ANOVA at significant = 0.01

Source of variation	SS	df	MS	F	$F_{cririca l}$
Between time	302.17	5	60.43	70.27	5.06
With in time	10.32	12	0.86		
total	312.49	17			

Table B7   A statistical test difference contact time (60 – 240 min) of Zn(II) by
using one-way ANOVA at significant = 0.01

Source of variation	SS	df	MS	F	$F_{cririca l}$
Between time	113.09	4	28.27	29.48	5.99
With in time	9.59	10	0.96		
total	122.68	14			

Table B8   A statistical test difference contact time (90 – 240 min) of Zn(II) by using one-way ANOVA at significant = 0.01

Source of variation	SS	df	MS	F	$F_{crirical}$
Between time	59.31	3	19.77	17.85	7.59
With in time	8.86	8	1.11		
total	68.17	11			

Table B9   A statistical test difference contact time (120 – 240 min) of Zn(II) by using one-way ANOVA at significant = 0.01

Source of variation	SS	df	MS	F	$F_{crirical}$
Between time	5.14	2	2.57	4.19	10.92
With in time	3.68	6	0.61		
total	8.82	8			

ศูนย์วิทยทรัพยากร
จุฬาลงกรณ์มหาวิทยาลัย

APPENDIX C

Effect of pH

Table C1 Effect of pH on the adsorption of Pb(II), Ni(II) and Zn(II) by AC-CoFe$_2$O$_4$

pH	Adsorbed amount of metal ions (mg/g)			% Removal		
	Pb(II)	Ni(II)	Zn(II)	Pb(II)	Ni(II)	Zn(II)
1	0.56 ± 0.48	0.09 ± 0.15	0.68 ± 0.31	1.00 ± 0.86	0.29 ± 0.50	3.37 ± 1.54
2	0.83 ± 0.83	0.26 ± 0.44	0.62 ± 0.35	1.47 ± 1.47	0.87 ± 1.51	3.03 ± 1.75
3	9.72 ± 0.96	0.26 ± 0.44	1.09 ± 0.31	17.41 ± 1.42	0.88 ± 1.52	5.39 ± 1.54
4	25.28 ± 1.27	0.60 ± 0.15	1.09 ± 0.12	45.27 ± 2.28	2.03 ± 0.50	5.67 ± 0.61
5	40.83 ± 0.83	2.05 ± 0.26	3.82 ± 0.24	73.13 ± 1.49	6.90 ± 0.86	19.86 ± 1.23
6	51.58 ± 0.14	6.07 ± 0.53	8.88 ± 0.12	95.23 ± 0.27	20.94 ± 1.84	47.62 ± 0.63

Mean ± S.D. (N=3)

Table C2 Percentage of leaching amount of Co and Fe from the composite compared
with the initial amount during adsorption of Pb(II), Ni(II) and Zn(II).

pH / Metal	Initial amount (mg g^{-1})		% Leaching					
	Co	Fe	Co			Fe		
			Pb	Ni	Zn	Pb	Ni	Zn
1			19.78	21.64	26.67	19.64	18.65	27.32
2			12.30	12.52	12.63	2.13	1.64	2.02
3	124.24	237.68	9.84	10.06	10.04	0.09	0.03	0.02
4			8.16	8.77	8.89	0.07	N.D.	N.D.
5			5.87	6.82	7.20	N.D.	N.D.	N.D.
6			3.07	3.63	4.21	N.D.	N.D.	N.D.

APPENDIX D

Adsorption kinetic and effect of adsorbent dosage

Table D1   Adsorption capacities (mg g^{-1}) for kinetic plot of Pb(II), Ni(II) and Zn(II) by AC-CoFe$_2$O$_4$

Metal		Pb	Ni	Zn
Weight (g)	Time (min)	Sorption capacity (mg g^{-1})	Sorption capacity (mg g^{-1})	Sorption capacity (mg g^{-1})
0.0100	5	27.58 ± 0.29	2.86 ± 0.10	2.77 ± 0.02
	10	28.83 ± 0.14	3.06 ± 0.05	2.89 ± 0.02
	15	33.33 ± 0.14	3.28 ± 0.05	2.95 ± 0.02
	20	34.58 ± 0.14	3.42 ± 0.00	3.21 ± 0.13
	30	35.08 ± 0.14	3.47 ± 0.05	3.33 ± 0.02
	60	35.58 ± 0.14	3.64 ± 0.05	3.40 ± 0.02
	90	35.50 ± 0.14	3.67 ± 0.00	3.41 ± 0.02
	120	35.58 ± 0.14	3.69 ± 0.05	3.42 ± 0.00
0.0200	5	22.33 ± 0.13	2.36 ± 0.02	1.98 ± 0.00
	10	23.29 ± 0.07	2.53 ± 0.02	2.04 ± 0.00
	15	23.83 ± 0.00	2.64 ± 0.02	2.08 ± 0.00
	20	24.25 ± 0.14	2.76 ± 0.02	2.09 ± 0.00
	30	24.50 ± 0.07	2.81 ± 0.02	2.11 ± 0.00
	60	25.00 ± 0.07	2.97 ± 0.02	2.13 ± 0.00
	90	25.04 ± 0.07	2.96 ± 0.00	2.13 ± 0.00
	120	25.04 ± 0.07	2.99 ± 0.02	2.13 ± 0.00
0.0400	5	12.19 ± 0.04	2.01 ± 0.01	1.10 ± 0.00
	10	12.50 ± 0.04	2.20 ± 0.01	1.11 ± 0.00
	15	12.52 ± 0.04	2.19 ± 0.00	1.11 ± 0.00
	20	12.50 ± 0.04	2.19 ± 0.01	1.11 ± 0.00
	30	12.50 ± 0.04	2.19 ± 0.01	1.11 ± 0.00
	60	12.54 ± 0.00	2.19 ± 0.00	1.11 ± 0.00
	90	12.50 ± 0.04	2.19 ± 0.01	1.11 ± 0.00
	120	12.52 ± 0.04	2.19 ± 0.00	1.11 ± 0.00

Mean ± S.D. (N=3)

APPENDIX E

Adsorption isotherms

Table E1   Adsorption capacities (mg g^{-1}) for adsorption isotherm of Pb(II), Ni(II) and Zn(II) by AC-CoFe$_2$O$_4$

Metal	Initial concentration C_i (mg L^{-1})	Equilibrium concentration C_e (mg L^{-1})	Adsorption capacity Q (mg g^{-1})
	55.83	15.00 ± 0.83	40.83 ± 0.83
	108.00	52.89 ± 0.77	55.11 ± 0.77
	164.00	99.33 ± 1.15	64.67 ± 1.15
Pb	218.67	141.33 ± 2.67	77.33 ± 2.67
	324.00	241.33 ± 2.31	82.67 ± 2.31
	345.00	283.33 ± 2.89	78.33 ± 2.89
	405.00	325.00 ± 0.00	80.00 ± 0.00
	4.80	1.78 ± 0.08	3.02 ± 0.08
	9.67	5.82 ± 0.04	3.84 ± 0.04
	14.93	10.22 ± 0.15	4.71 ± 0.15
	20.33	15.06 ± 0.19	5.28 ± 0.19
	25.11	19.41 ± 0.13	5.70 ± 0.13
Ni(II)	28.97	22.91 ± 0.53	6.07 ± 0.53
	45.98	39.88 ± 0.26	6.10 ± 0.26
	92.86	85.42 ± 1.03	7.44 ± 1.03
	141.43	133.81 ± 0.82	7.62 ± 0.82
	189.29	181.55 ± 1.03	7.74 ± 1.03

Table E1 (continued)

Metal	Initial concentration C_i (mg L^{-1})	Equilibrium concentration C_e (mg L^{-1})	Adsorption capacity Q (mg g^{-1})
	0.93	0.08 ± 0.00	0.85 ± 0.00
	4.57	0.93 ± 0.06	3.64 ± 0.06
	9.07	3.44 ± 0.07	5.63 ± 0.07
Zn	13.51	6.49 ± 0.13	7.02 ± 0.13
	18.65	9.77 ± 0.12	8.88 ± 0.12
	48.86	36.68 ± 0.25	12.18 ± 0.25
	75.35	61.03 ± 0.41	14.32 ± 0.41
	93.31	80.11 ± 0.00	13.20 ± 0.00
	138.50	124.41 ± 1.17	14.08 ± 1.17

Mean $\pm$ S.D. (N=3)

APPENDIX F

Effect of salts

Table F1 Effect of salts on the Pb(II), Ni(II) and Zn(II) ions adsorption by
AC-CoFe$_2$O$_4$

Metal	Adsorbed amount of metal (mg/g)						
	No salt	Type of salts					
		NaNO$_3$		Ca(NO$_3$)$_2$		Na$_2$SO$_4$	
		0.1 M	1 M	0.1 M	1 M	0.1 M	1 M
Pb(II)	32.22 ± 1.11	31.85 ± 0.64	27.41 ± 0.64	28.15 ± 0.64	20.74 ± 0.64		
Ni(II)	9.49 ± 0.44	8.55 ± 0.30	8.12 ± 0.15	4.19 ± 0.15	5.90 ± 0.26	7.78 ± 0.30	7.26 ± 0.15
Zn(II)	3.76 ± 0.04	3.35 ± 0.00	2.91 ± 0.04	2.13 ± 0.00	2.13 ± 0.06	3.19 ± 0.04	1.97 ± 0.04

Mean ± S.D. (N=3)

VITA

Miss Pattarporn Numsrinirun was born on May 17, 1986 in Bangkok, Thailand. After completing her high school from Satri-sri-su-ri-yo-thai School, she entered the Department of Chemistry, Faculty of Science, Chulalongkorn University in 2004. She received her Bachelor of Science Degree in March 2008. Then, she continued her graduate study at the same university and become a member of Environmental Analysis Research Unit under the supervision of Assistant Professor Fuangfa Unob. In 5-7 January 2011, she attended Pure and Applied Chemistry International Conference in the title of "Removal of toxic metal by activated carbon-$CoFe_2O_4$ magnetic composites" by poster presentation. She finished her postgraduate study with the Master degree of Science in 2011. Her present address is 30 Soi Chan 16, Thanurat Road, Sathon, Bangkok, 10120 Thailand. Contact number is 083-715-2772.